

# Efficient LLR-Domain Decoding of ABS+ Polar Codes

Mikhail Chernikov, Peter Trifonov

**Abstract**—ABS+ polar codes are a generalization of Arikan polar codes that provides much faster polarization. We present an LLR-domain implementation of the SCL decoder of ABS+ polar codes. Furthermore, we optimize the SCL algorithm in order to reduce the complexity requirements for the LLRs computation. In comparison with classical polar codes, the proposed approach requires less number of arithmetic operations in the SCL decoder to obtain the fixed frame error rate (FER) at high-SNR region.

**Index Terms**—Polar codes, log-likelihood ratio, fast decoding, successive cancellation decoding.

## I. INTRODUCTION

POLAR codes [1] achieve the capacity of a binary memoryless channel under successive cancellation (SC) decoding in the case of an infinite length. This decoder exploits the channel polarization phenomenon. Namely, polar encoding procedure gives rise to virtual subchannels that converge to either pure-noisy or pure-noiseless state. However, in the finite-length regime, the performance of SC is very poor. To overcome this issue one can use successive cancellation list (SCL) decoder [2] which maintains a list of most likely prefixes of a message vector. Together with a cyclic redundancy check (CRC), SCL decoder demonstrates excellent error-correcting performance which is comparable to that of LDPC and turbo codes.

The complexity of a hardware implementation of the SCL decoder crucially depends on the list size [3]. For a moderate blocklength the SCL decoder attains maximum likelihood (ML) even if the list size is pretty small. However, when the length is growing, the list size, required to get the near ML performance, increases exponentially [4]. This results in very restricted applicability of polar codes in practical systems. Several alternative decoding algorithms were recently proposed: sequential decoding [5], SC flip and perturbation decoding [6], sphere decoding [7], belief propagation [8] decoding and permutation-based decoding [9]. But, all these algorithms either are even more complicated or provide worse performance than SCL. So, at the current moment SCL algorithm is state-of-the-art solution for polar codes.

The exponential increase of the required list size takes place since classical polar codes are suboptimal. More precisely, for a finite code length there are many virtual subchannels which are far away from the polarized state. They lead to a significant gap between the capacity of the underlying physical channel and the rate of the polar code which uses only reliable subchannels to transmit an input message. There were invented other polarizing transforms, such that the corresponding virtual subchannels converge to the polarized state much faster. The most studied way is to replace the Arikan kernel

$$F = \begin{pmatrix} 1 & 0 \\ 1 & 1 \end{pmatrix} \quad (1)$$

with some other binary square non-singular kernel matrix. The resulting codes are referred to as polar codes with large kernels [10]. There are explicit methods for kernel constructing that provide substantially better scaling exponent [11]. Moreover, some specific kernels were shown to enable low-complexity decoding under window processing (WP) algorithm [12], [13].

Another generalization of Arikan polar codes are recently discovered Adjacent-Bit-Swapped (ABS) [14] and ABS+ polar codes [15]. The encoding procedure is similar to encoding of polar codes with Arikan kernel, but to deepen the polarization, specific additional transforms of some adjacent bits are performed. Due to the similarity to classical polar codes up to those transforms, ABS and ABS+ polar codes can be decoded by the decoder, analogous to the classical SC or SCL.

In this paper, we present the version of the SCL decoder for ABS+ polar codes that performs calculations over log-likelihood ratios (LLRs) instead of transition probabilities. This decoder uses only addition and comparison operations over real numbers what is necessary for an efficient hardware implementation [16]. Moreover, we conjecture that lots of calculations in the originally presented SC algorithm are redundant. Indeed, at each phase it computes probabilities of two next message bits to be 0 or 1. However, it decodes only one bit dropping out the probabilities for the second one. Inspired by this idea, we provide a new version of the SC decoder (that can be easily generalized to SCL) not performing such unnecessary computations.

The proposed approach is compared against SCL decoder applied to classical polar codes. The numeric results show that for a fixed list size in the SCL decoder ABS+ codes demonstrate noticeably better performance. Besides, in many cases ABS+ decoder outperforms the standard one when the number of arithmetic operations in both decoders is fixed. Moreover, the loss of the proposed decoder to the probability-domain decoder from [15] is negligible.

The rest of this paper is organized as follows. In Section II the necessary background about classical and ABS+ polar codes is given. In Section III the LLR-domain decoder of ABS+ polar codes is proposed. Section IV describes simulation results. Finally, takeaways and suggestions for a future work are discussed in Section V.

## II. BACKGROUND

In this paper, the notation  $x_i^j$  is used for the following subvector of  $x$ :  $x_i^j = (x_i, x_{i+1}, \dots, x_j)$ . We also use  $x_{i,o}^j$  and  $x_{i,e}^j$  to denote the subvectors consisting of entries with only odd and only even indices respectively. Vectors are indexed from one. For a channel  $W$  the notation  $W : \mathcal{X} \rightarrow \mathcal{Y}$  defines  $\mathcal{X}$  and  $\mathcal{Y}$  as input and output alphabets of  $W$ . The corresponding probability density function is denoted by

$W(y|x)$ ,  $x \in \mathcal{X}$ ,  $y \in \mathcal{Y}$ . Kronecker product of matrices  $A$  and  $B$  is denoted by  $A \otimes B$ ,  $A^{\otimes m}$  corresponds to the  $m$ th Kronecker power of  $A$ . All operations over binary values are performed modulo two.

### A. Classical polar codes

A polar code is a binary linear block code whose codewords are vectors  $uF^{\otimes m}$ , where  $n = 2^m$  is the length,  $F$  is defined in (1) and  $u$  is an  $n$ -dimensional binary vector having zeros at all the positions from the predefined set  $\mathcal{F} \subseteq \{1, 2, \dots, n\}$  called frozen set. In what follows the vector  $u$  is referred to as a message vector and  $n = 2^m$  is reserved for code length.

Multiplying by  $G_m = F^{\otimes m}$  results in the channel polarization effect [1]. Consider a binary discrete memoryless channel (B-DMC)  $W : \{0, 1\} \rightarrow \mathcal{Y}$  with transition probability function  $W(y|x)$ . Let us transmit entries of a vector  $uG_m$  through  $n$  independent copies of  $W$ . This gives rise to  $n$  virtual bit subchannels  $\mathbf{W}_i^{(m)} : \{0, 1\} \rightarrow \mathcal{Y}^n \times \{0, 1\}^{i-1}$ ,  $1 \leq i \leq n$  with transition probabilities

$$\mathbf{W}_i^{(m)}(y_1^n, u_1^{i-1}|u_i) = \frac{1}{2^{n-1}} \sum_{u_{i+1}^n \in \{0, 1\}^{n-i}} \mathbf{W}^{(m)}(y_1^n|u_1^n), \quad (2)$$

where  $\mathbf{W}^{(m)}(y_1^n|u_1^n) = \prod_{j=1}^n W(y_j|(u_1^n G_m)_j)$  is the probability to receive the vector  $y_1^n$  if  $u_1^n G_m$  has been transmitted.

When  $n$  grows to infinity, every subchannel becomes either absolutely noisy or absolutely noiseless. In order to transmit information in the most efficient way, indices of the least reliable bit subchannels are included to  $\mathcal{F}$ . The remaining positions of the message vector are called information and they are used to carry payload.

### B. Successive cancellation decoding

The SC decoding algorithm sequentially estimates bits of the message vector. If the  $i$ th bit, it calculates the transition probabilities of the corresponding virtual subchannel with respect to the received vector  $y_1^n$  and previously decoded message bits  $\hat{u}_1^{i-1}$ . Then, it makes the hard decision:

$$\hat{u}_i = \begin{cases} \operatorname{argmax}_{u_i \in \{0, 1\}} \mathbf{W}_i^{(m)}(y_1^n, \hat{u}_1^{i-1}|u_i), & i \notin \mathcal{F}, \\ 0, & \text{otherwise.} \end{cases} \quad (3)$$

After all message bits are decoded, the corresponding codeword  $\hat{c}_1^n = \hat{u}_1^n G_m$  is returned.

The procedure of calculation of these transition probabilities can be seen as a binary tree traversal (for example, see [17, Fig. 1]). In fact, there is a recursive relation between virtual subchannels. Consider the polarizing transform depicted in Fig. 1. Here we pass the result, i.e.  $(u_1 + u_2, u_2)$ , through two independent copies of a B-DMC  $W : \{0, 1\} \rightarrow \mathcal{Y}$ . This leads to the virtual channels  $W^- : \{0, 1\} \rightarrow \mathcal{Y}^2$  and  $W^+ : \{0, 1\} \rightarrow \mathcal{Y}^2 \times \{0, 1\}$  such that

$$W^-(y_1, y_2|u_1) = \frac{1}{2} \sum_{u_2 \in \{0, 1\}} W(y_1|u_1 + u_2)W(y_2|u_2), \quad (4a)$$

$$W^+(y_1, y_2, u_1|u_2) = \frac{1}{2} W(y_1|u_1 + u_2)W(y_2|u_2). \quad (4b)$$

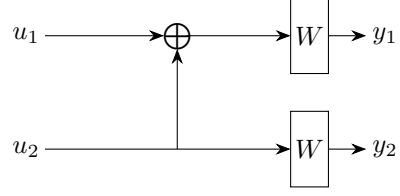


Fig. 1: Polarization of a channel  $W : \{0, 1\} \rightarrow \mathcal{Y}$ .

Then, for every  $1 \leq i \leq 2^{m-1}$  one has

$$\mathbf{W}_{2i-1}^{(m)} = \left( \mathbf{W}_i^{(m-1)} \right)^-, \quad \mathbf{W}_{2i}^{(m)} = \left( \mathbf{W}_i^{(m-1)} \right)^+. \quad (5)$$

To make the computations hardware-friendly, the transition probabilities can be replaced with approximate LLRs for the corresponding virtual subchannels [18]. We define the approximate LLRs as follows:

$$\mathbf{S}_i^{(m)}(y_1^n, u_1^{i-1}) = \ln \frac{\tilde{\mathbf{W}}_i^{(m)}(y_1^n, u_1^{i-1}|0)}{\tilde{\mathbf{W}}_i^{(m)}(y_1^n, u_1^{i-1}|1)}, \quad (6)$$

where  $1 \leq i \leq n$  and

$$\tilde{\mathbf{W}}_i^{(m)}(y_1^n, u_1^{i-1}|u_i) = \max_{u_{i+1}^n \in \{0, 1\}^{n-i}} \mathbf{W}^{(m)}(y_1^n|u_1^n) \quad (7)$$

is the approximation of the transition probability of  $\mathbf{W}_i^{(m)}$ . For the computation of the approximate LLRs, the decoder apply the following relation recursively:

$$\mathbf{S}_{2i-1}^{(m)}(y_1^n, u_1^{2i-2}) = f_-(a, b) \triangleq \operatorname{sgn}(a) \operatorname{sgn}(b) \min\{|a|, |b|\}, \quad (8a)$$

$$\mathbf{S}_{2i}^{(m)}(y_1^n, u_1^{2i-1}) = f_+(a, b, u_{2i-1}) \triangleq (-1)^{u_{2i-1}} a + b, \quad (8b)$$

where  $a = \mathbf{S}_i^{(m-1)}(y_{1,o}^n, u_{1,o}^{2i-2} + u_{1,e}^{2i-2})$ ,  $b = \mathbf{S}_i^{(m-1)}(y_{1,e}^n, u_{1,e}^{2i-2})$ . The initial values are  $\mathbf{S}_1^{(0)}(y_\beta) = \ln \frac{W(y_\beta|0)}{W(y_\beta|1)}$ ,  $1 \leq \beta \leq n$ . The hard decisions are made with accordance to the signs of the LLRs:

$$\hat{u}_i = \begin{cases} 1, & \mathbf{S}_i^{(m)}(y_1^n, \hat{u}_1^{i-1}) < 0 \text{ and } i \notin \mathcal{F}, \\ 0, & \text{otherwise.} \end{cases} \quad (9)$$

### C. Successive cancellation list decoding

Although SC decoding allows polar codes to achieve theoretical limits for  $n \rightarrow \infty$ , for finite  $n$  its performance is far away from the maximum likelihood (ML). Polar codes can be decoded near ML by using the SCL algorithm [2], a modification of the standard SC decoding. We are to review its LLR-based version [16] which is considered as the most appropriate solution for a practical usage at the current moment.

The SCL algorithm maintains up to  $L$  possible prefixes of the message vector which are referred to as paths. Here  $L$  is the predefined parameter called list size. The decoder recursively computes the values  $\mathbf{S}_i^{(m)}(y_1^n, \hat{u}_1^{i-1})$  for each path (so, here  $\hat{u}_1^{i-1}$  denotes message bits of some considered path) in the same way as in SC. If  $i \in \mathcal{F}$ , all paths are being continued with  $\hat{u}_i = 0$ . Otherwise, the decoder splits every path into two continuations with  $\hat{u}_i = 0$  and  $\hat{u}_i = 1$ . After that, some least

likely paths are eliminated in order to get at most  $L$  paths present in the list.

To determine a path likelihood after the  $i$ th message bit has been processed, the decoder computes for each active path  $l$  the number  $\text{PM}_i^{(l)}$  called path metric (PM). Greater metric corresponds to a less reliable path. Initially there are only one active path whose metric is zero. The PMs are being updated as

$$\text{PM}_i^{(l')} = \begin{cases} \text{PM}_{i-1}^{(l)}, & \hat{u}_i = \frac{1}{2}(1 - \text{sgn}(\alpha)), \\ \text{PM}_{i-1}^{(l)} + |\alpha|, & \text{otherwise,} \end{cases} \quad (10)$$

where  $\alpha = S_i^{(m)}(y_1^n, \hat{u}_1^{i-1})$ ,  $\hat{u}_1^{i-1}$  are message bits of the  $l$  path and  $l'$  is the index of the path representing the continuation of the  $l$ th one with  $\hat{u}_i$ . Saying less formally, each path is penalized when its hard decision does not match the sign of the LLR. As the result, the decoder returns the codeword corresponding to the most reliable path after all  $n$  message bits are decoded.

#### D. ABS+ polar codes

For  $n \rightarrow \infty$  the capacity of every virtual channel in (2) tends either to 0 or to 1 [1], but for a moderate code length there are many subchannels that are not fully polarized, i.e. whose capacities belong to the interval  $(\delta, 1-\delta)$  for some sufficiently large  $\delta \in (0, \frac{1}{2})$ . This may result in a poor performance of the SC decoder or the SCL decoder with not sufficiently large list size. To deepen the polarization in the finite-length regime, authors in [14] and [15] have suggested to perform specific transforms over adjacent bits while encoding. This gives rise to virtual subchannels that achieve the polarized state, when  $n$  is growing, provably faster than the channels in (2). Therefore, polar codes based on this idea (called ABS+ polar codes [15]) provide substantially better SC/SCL decodability with respect to the classical ones.

The polarization matrix of a classical polar code is defined as  $G_m = G_{m-1} \otimes F$ . When it comes to an ABS+ polar code, we have matrix  $G_m^{\text{ABS}+} = Q_m^{\text{ABS}+}(G_{m-1}^{\text{ABS}+} \otimes F)$  with the initial condition  $G_1^{\text{ABS}+} = F$ , where  $Q_m^{\text{ABS}+}$  is the  $n \times n$  matrix, corresponding to the mentioned transforms of adjacent bits. Namely,  $Q_m^{\text{ABS}+}$  is defined by two sets  $\mathcal{I}_S^{(m)}, \mathcal{I}_A^{(m)} \subseteq \{1, 2, \dots, n-1\}$  and is represented as

$$Q_m^{\text{ABS}+} = \left( \prod_{i \in \mathcal{I}_S^{(m)}} S_m(i) \right) \left( \prod_{i \in \mathcal{I}_A^{(m)}} A_m(i) \right), \quad (11)$$

where  $S_m(i)$  and  $A_m(i)$  are  $n \times n$  binary matrices such that for every  $x \in \{0, 1\}^n$  one has

- 1)  $xS_m(i) = (x_1, \dots, x_{i-1}, x_{i+1}, x_i, x_{i+2}, \dots, x_n)$ ,
- 2)  $xA_m(i) = (x_1, \dots, x_{i-1}, x_i + x_{i+1}, x_{i+1}, \dots, x_n)$ .

In the first case we have entries  $x_i$  and  $x_{i+1}$  swapped and in the second case we have  $x_{i+1}$  added to  $x_i$  while the other elements of  $x$  are kept unchanged. Furthermore, the sets  $\mathcal{I}_S^{(m)}$  and  $\mathcal{I}_A^{(m)}$  must satisfy two following constraints:

- (i)  $\mathcal{I}_S^{(m)} \cap \mathcal{I}_A^{(m)} = \emptyset$ .
- (ii) Let  $\mathcal{I}^{(m)} = \mathcal{I}_S^{(m)} \cup \mathcal{I}_A^{(m)} = \{i_1, i_2, \dots, i_s\}$ . Then

$$i_1 + 4 \leq i_2, i_2 + 4 \leq i_3, \dots, i_{s-1} + 4 \leq i_s.$$

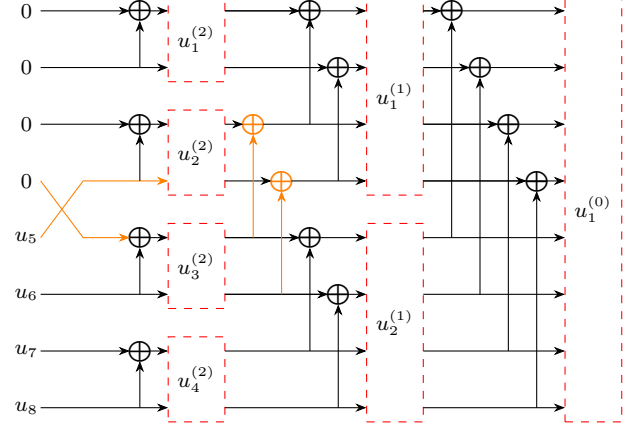


Fig. 2: Circuit for the  $(8, 4)$  ABS+ polar code with  $\mathcal{F} = \{1, 2, 3, 4\}$ ,  $\mathcal{I}_S^{(3)} = \{4\}$ ,  $\mathcal{I}_A^{(3)} = \emptyset$ ,  $\mathcal{I}_S^{(2)} = \emptyset$ ,  $\mathcal{I}_A^{(2)} = \{2\}$ . Additional transforms of adjacent bits are highlighted.

Of course, these conditions are also held for all  $Q_\lambda^{\text{ABS}+}$ ,  $2 \leq \lambda < m$ . So, an ABS+ polar code is defined by a frozen set  $\mathcal{F} \subseteq \{1, 2, \dots, n\}$  and sets  $\{\mathcal{I}_S^{(\lambda)}, \mathcal{I}_A^{(\lambda)}\}_{\lambda=2}^m$  and the codewords have the form  $uG_m^{\text{ABS}+}$ , where  $u \in \{0, 1\}^n$  is a message vector obtained in the same way as for classical polar codes.

The matrix  $Q_m^{\text{ABS}+}$  is being chosen in the way that leads to fastest polarization if multiplication of a message vector by  $Q_m^{\text{ABS}+}(G_{m-1}^{\text{ABS}+} \otimes F)$  is considered. In [15] the authors formulate the corresponding optimization problem and propose an explicit algorithm solving it. In that work, it is also noticed that for the purpose of deepening polarization by using transforms of adjacent bits, it is sufficient to take into account only transforms  $S_m(i)$  and  $A_m(i)$  for all  $1 \leq i \leq n-1$ . Moreover, a transformation over the  $i$ th and  $i+1$ th bit may improve polarization only for  $i$  having the form  $i = 2j$ . Hence, all elements of  $\mathcal{I}^{(m)}$  are even numbers.

Let us describe the encoding of ABS+ polar codes more precisely. For this we need to review the standard polar encoding procedure, i.e. multiplication by  $F^{\otimes m}$ . This can be interpreted as a sequential application of  $m$  so called polarization layers. For input bits  $u_1^n$  let  $u_{i,1}^{(m)} = u_i$ ,  $1 \leq i \leq n$ . Next, for  $1 \leq \lambda < m$ ,  $1 \leq i \leq 2^\lambda$ ,  $N = 2^{m-\lambda}$  consider  $u_i^{(\lambda)} = (u_{i,1}^{(\lambda)}, \dots, u_{i,N}^{(\lambda)})$ :

$$u_i^{(\lambda)} = (u_{2i-1}^{(\lambda+1)} + u_{2i}^{(\lambda+1)} \mid u_{2i}^{(\lambda+1)}). \quad (12)$$

We number the layers from  $m-1$  to 0. After the  $\lambda$ th layer has been performed, the initial vector is transformed to  $(u_1^{(\lambda)} \mid u_2^{(\lambda)} \mid \dots \mid u_{2^\lambda}^{(\lambda)})$ . Then,  $u_1^{(0)}$  is the resulting codeword. In the case of ABS+ polar codes the encoding scheme can be represented in the analogous way up to performing additional operations between the polarization layers. For  $2 \leq \lambda \leq m$  and  $1 \leq \beta \leq N$  consider multiplication of  $(u_{1,\beta}^{(\lambda)}, u_{2,\beta}^{(\lambda)}, \dots, u_{2^{\lambda},\beta}^{(\lambda)})$  by  $Q_\lambda^{\text{ABS}+}$ . This is a sequence of multiplications by  $S_\lambda(i)$ ,  $i \in \mathcal{I}_S^{(\lambda)}$  and multiplications by  $A_\lambda(i)$ ,  $i \in \mathcal{I}_A^{(\lambda)}$ . Multiplication by  $S_\lambda(i)$  applied for all  $1 \leq \beta \leq N$  corresponds to swapping  $u_i^{(\lambda)}$  and  $u_{i+1}^{(\lambda)}$ . Multiplication by  $A_\lambda(i)$  corresponds to replacing  $u_i^{(\lambda)}$  with  $u_i^{(\lambda)} + u_{i+1}^{(\lambda)}$ . So, recalling that all such  $i$  are even numbers, instead of (12), one has the following relation:

$$u_i^{(\lambda)} = \begin{cases} (u_{2i-1}^{(\lambda+1)} + u_{2i}^{(\lambda+1)} \mid u_{2i}^{(\lambda+1)}), \\ 2i \notin \mathcal{I}^{(\lambda+1)}, 2(i-1) \notin \mathcal{I}_S^{(\lambda+1)} & (13a) \\ (u_{2i-2}^{(\lambda+1)} + u_{2i}^{(\lambda+1)} \mid u_{2i}^{(\lambda+1)}), \\ 2(i-1) \in \mathcal{I}_S^{(\lambda+1)}, & (13b) \\ (u_{2i-1}^{(\lambda+1)} + u_{2i+1}^{(\lambda+1)} \mid u_{2i+1}^{(\lambda+1)}), 2i \in \mathcal{I}_S^{(\lambda+1)}, & (13c) \\ (u_{2i-1}^{(\lambda+1)} + u_{2i}^{(\lambda+1)} + u_{2i+1}^{(\lambda+1)} \mid \\ u_{2i}^{(\lambda+1)} + u_{2i+1}^{(\lambda+1)}), 2i \in \mathcal{I}_A^{(\lambda+1)}, & (13d) \end{cases}$$

An example of the encoding circuit for an ABS+ polar code is given in Fig. 2.

### E. SC decoding of ABS+ polar codes in the probability domain

The SC decoder of ABS+ polar subcodes also sequentially decodes message bits considering the virtual subchannels. More precisely, similarly to (2), one can introduce the channels

$$\mathbf{W}_i^{(m),\text{ABS}^+}(y_1^n, u_1^{i-1} \mid u_i) = \frac{1}{2^{n-1}} \sum_{u_{i+1}^n \in \{0,1\}^{n-i}} \mathbf{W}^{(m),\text{ABS}^+}(y_1^n \mid u_1^n). \quad (14)$$

with  $\mathbf{W}^{(m),\text{ABS}^+}(y_1^n \mid u_1^n) = \prod_{j=1}^n W(y_j \mid (u_1^n G_m^{\text{ABS}^+})_j)$ . However, between these subchannels there does not exist an explicit recursive relation (analogous to (5)) that could be used by the decoder.

Instead, one can consider double-bit-input (DBI) virtual subchannels  $\mathbf{V}_i^{(m),\text{ABS}^+} : \{0,1\}^2 \rightarrow \mathcal{Y}^n \times \{0,1\}^{i-1}$ ,  $1 \leq i < n$  whose input represents two adjacent bits (the  $i$ th and the  $(i+1)$ th one) of a message vector and the output is the preceding prefix of the message vector together with received values from the copies of  $W$ . Lemma 3 from [15] establishes a recursive relation between these channels for computating of the transition probabilities.

Before we explore the decoding algorithm, let us introduce some notations. We use  $y_1^n \in \mathcal{Y}^n$  to denote a received vector,  $\hat{u}_i$  is estimation of the  $i$ th bit and  $\hat{u}_i^{(\lambda)}$  is estimation of  $u_i^{(\lambda)}$  from (13). We also use the shortcut

$$\hat{x}_{i,\beta}^{(\lambda)} = (y_\beta, y_{\beta+N}, \dots, y_{\beta+(2^\lambda-1)N}, \hat{u}_{1,\beta}^{(\lambda)}, \hat{u}_{2,\beta}^{(\lambda)}, \dots, \hat{u}_{i-1,\beta}^{(\lambda)})$$

with  $0 \leq \lambda \leq m$ ,  $1 \leq i \leq 2^\lambda$ ,  $1 \leq \beta \leq N = 2^{m-\lambda}$ .

Note that for  $1 \leq \lambda \leq m$  and  $1 \leq i \leq 2^\lambda$  such that  $2i \in \mathcal{I}^{(\lambda+1)}$ , in order to get  $u_i^{(\lambda)}$ , the vectors  $u_{2i-1}^{(\lambda+1)}$ ,  $u_{2i}^{(\lambda+1)}$ ,  $u_{2i+1}^{(\lambda+1)}$  must be decoded (see (13c) and (13d)). Moreover, according to [15, Lemma 3], in these cases the calculation of the transition probabilities of  $\mathbf{V}_{2i+1}^{(\lambda+1),\text{ABS}^+}$  is based on the transition probabilities of  $\mathbf{V}_i^{(\lambda),\text{ABS}^+}$ . The SC decoder of classical polar codes, in contrast, recursively processes only the  $(2i-1)$ th and the  $(2i)$ th channels to decode  $u_i^{(\lambda)}$ . Another point to mention is that there are only  $n-1$  virtual subchannels. So,  $n$ th message bit is being decoded together with the  $(n-1)$ th one. The last remark is that sometimes message bits that are being estimated while decoding  $u_{i-1}^{(\lambda)}$  are also needed to obtain  $u_i^{(\lambda)}$ . Namely, if

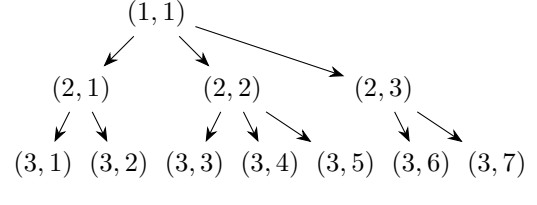


Fig. 3: The tree of the recursion in the SC algorithm applied to an ABS+ polar code with  $\mathcal{I}_S^{(2)} = \emptyset$ ,  $\mathcal{I}_A^{(2)} = \{1\}$ ,  $\mathcal{I}_S^{(3)} = \{4\}$ ,  $\mathcal{I}_A^{(3)} = \emptyset$ .

$2(i-1) \in \mathcal{I}^{(\lambda+1)}$ ,  $\hat{u}_i^{(\lambda)} = (v + u_{2i}^{(\lambda+1)} \mid u_{2i}^{(\lambda+1)})$ , where  $v$  is already decoded before decoding  $u_i^{(\lambda)}$ . So,  $v$  is being stored in a specific buffer after it has been decoded and is copied when it is necessary to calculate  $u_i^{(\lambda)}$ .

The decoding consists of recursive computation of transition probabilities for the virtual DBI channels, making hard decisions and obtaining the resulting codeword by application of (13) to estimated message bits. The recursion can be seen as a traversal of a tree which represents dependencies between virtual DBI channels and intermediate vectors in (13). An example of such tree is depicted in Fig. 3. Every node is labeled by a pair of integers  $(\lambda, i)$  such that  $1 \leq \lambda \leq m$ ,  $1 \leq i \leq 2^\lambda - 1$ . Here  $\lambda$  is referred to as number of layer,  $i$  is referred to as number of phase. The node  $(1, 1)$  is the tree root. Leafs are the nodes from the  $m$ th layer. All edges have the form  $(\lambda, i) \rightarrow (\lambda+1, j)$ , where  $j \in \{2i-1, 2i, 2i+1\}$ . The edge  $(\lambda, i) \rightarrow (\lambda+1, j)$  indicates that  $\mathbf{V}_j^{(\lambda+1),\text{ABS}^+}$  can be obtained by applying one of the transforms  $(-)^\nabla, (-)^\diamond, (-)^\Delta, (-)^\nabla, (-)^\diamond, (-)^\Delta, (-)^\nabla, (-)^\diamond, (-)^\Delta$  (see [15]) to  $\mathbf{V}_i^{(\lambda),\text{ABS}^+}$ . As the input for processing of the node  $(\lambda, i)$  the algorithm receives the array of values  $\mathbf{V}_i^{(\lambda),\text{ABS}^+}(\hat{x}_{i,\beta}^{(\lambda)} \mid a, b)$ ,  $1 \leq \beta \leq 2^{m-\lambda}$ ,  $a, b \in \{0,1\}$ . As the output, it returns  $\hat{u}_i^{(\lambda)}$  and, if  $i = 2^\lambda - 1$ ,  $\hat{u}_{i+1}^{(\lambda)}$  is also returned. To process the leaf node  $(m, i)$ , the algorithm makes a hard decision on  $u_i$  using

$$\mathbf{W}_i^{(m),\text{ABS}^+}(y_1^n, u_1^{i-1} \mid u_i) = \frac{1}{2} \sum_{u_{i+1}^n \in \{0,1\}} \mathbf{V}_i^{(m),\text{ABS}^+}(y_1^n, u_1^{i-1} \mid u_i, u_{i+1}),$$

$$\mathbf{W}_{i+1}^{(m),\text{ABS}^+}(y_1^n, u_1^i \mid u_{i+1}) = \frac{1}{2} \mathbf{V}_i^{(m),\text{ABS}^+}(y_1^n, u_1^{i-1} \mid u_i, u_{i+1}).$$

If  $i = n-1$ ,  $u_{i+1}$  is also decoded. Non-leaf nodes are being processed by recursive visiting of the child nodes in the ascending order of the phases. The transition probabilities for children of  $(\lambda, i)$  are being computed with respect to the known values  $\mathbf{V}_i^{(\lambda),\text{ABS}^+}(\hat{x}_{i,\beta}^{(\lambda)} \mid a, b)$ ,  $1 \leq \beta \leq 2^{m-\lambda}$ ,  $a, b \in \{0,1\}$  and the previously decoded bits on the  $(\lambda+1)$ th layer. The resulting vector  $\hat{u}_i^{(\lambda)}$  is being calculated with respect to the results of children processing (and the value stored at the  $i-1$  phase if  $2(i-1) \in \mathcal{I}^{(\lambda+1)}$ ). The initial probabilities for processing of the root node are

$$\mathbf{V}_1^{(1),\text{ABS}^+}(y_\beta, y_{\beta+N/2} \mid a, b) = W(y_\beta \mid a+b)W(y_{\beta+N/2} \mid b).$$

The resulting codeword can be easily obtained from the vectors  $\hat{u}_1^{(1)}, \hat{u}_2^{(1)}$  representing the output after processing of the root.

### III. LLR-DOMAIN COMPUTATIONS FOR DECODING OF ABS+ POLAR CODES

As established in [16] and [18], a hardware implementation of SC-like decoders can be significantly simplified by using LLRs instead of transition probabilities. In the case of ABS+ polar codes calculations of these probabilities are even more complicated than for classical polar codes. Hence, it is necessary to adapt the decoder to LLR domain.

We start from the definitions of virtual channels that approximate (14) in Section III-A. As in (7), our approximate probabilities correspond to the most likely continuation of a message vector. Then we establish a recursive relation between approximate DBI channels and present the formulas for evaluation of the LLRs. In Section III-B and Section III-C we analyse these formulas and suggest heuristics for their application in a low-complexity way. In Section III-D we formulate the efficient SC decoding algorithm in the LLR domain. Generalization of this SC decoder to SCL is briefly discussed in Section III-E.

#### A. Evolution of the approximate LLRs

Similarly to (7), we define the approximate probabilities for the virtual bit subchannels

$$\tilde{\mathbf{W}}_i^{(m),\text{ABS}+}(y_1^n, u_1^{i-1}|u_i) = \max_{u_{i+1} \in \{0,1\}^{n-i}} \mathbf{W}^{(m),\text{ABS}+}(y_1^n|u_1^n) \quad (15)$$

with  $1 \leq i \leq n$  and also for the defined earlier DBI subchannels:

$$\begin{aligned} \tilde{\mathbf{V}}_i^{(m),\text{ABS}+}(y_1^n, u_1^{i-1}|u_i, u_{i+1}) &= \\ &= \max_{u_{i+2} \in \{0,1\}^{n-i-1}} \mathbf{W}^{(m),\text{ABS}+}(y_1^n|u_1^n) \end{aligned} \quad (16)$$

with  $1 \leq i < n$ . By definition one has

$$\begin{aligned} \tilde{\mathbf{W}}_i^{(m),\text{ABS}+}(y_1^n, u_1^{i-1}|u_i) &= \max_{u_{i+1} \in \{0,1\}^{n-i}} \mathbf{W}^{(m),\text{ABS}+}(y_1^n|u_1^n) \\ &= \max_{u_{i+1} \in \{0,1\}} \max_{u_{i+2} \in \{0,1\}^{n-i-1}} \mathbf{W}^{(m),\text{ABS}+}(y_1^n|u_1^n) \\ &= \max_{u_{i+1} \in \{0,1\}} \tilde{\mathbf{V}}_i^{(m),\text{ABS}+}(y_1^n, u_1^{i-1}|u_i, u_{i+1}), \end{aligned} \quad (17a)$$

$$\tilde{\mathbf{W}}_{i+1}^{(m),\text{ABS}+}(y_1^n, u_1^i|u_{i+1}) = \tilde{\mathbf{V}}_i^{(m),\text{ABS}+}(y_1^n, u_1^{i-1}|u_i, u_{i+1}) \quad (17b)$$

establishing the relation between the single- and double-bit virtual channels. Next, for  $1 \leq i < n$  let us define LLRs for these approximate probabilities:

$$\mathbf{L}_i^{(m)}(y_1^n, u_1^{i-1}) = \ln \frac{\max_{b \in \{0,1\}} \tilde{\mathbf{V}}_i^{(m),\text{ABS}+}(y_1^n, u_1^{i-1}|b, 0)}{\max_{b \in \{0,1\}} \tilde{\mathbf{V}}_i^{(m),\text{ABS}+}(y_1^n, u_1^{i-1}|b, 1)}, \quad (18a)$$

$$\mathbf{R}_i^{(m)}(y_1^n, u_1^{i-1}; b) = \ln \frac{\tilde{\mathbf{V}}_i^{(m),\text{ABS}+}(y_1^n, u_1^{i-1}|b, 0)}{\tilde{\mathbf{V}}_i^{(m),\text{ABS}+}(y_1^n, u_1^{i-1}|b, 1)}, \quad b \in \{0, 1\}. \quad (18b)$$

So, instead of computing  $\mathbf{V}_i^{(m),\text{ABS}+}(\hat{x}_{i,\beta}^{(\lambda)}|a, b)$ ,  $a, b \in \{0, 1\}$  for  $1 \leq i < n$  and  $1 \leq \beta \leq 2^{m-\lambda}$ , the proposed decoder

maintains three real numbers  $\mathbf{L}_i^{(\lambda)}(\hat{x}_{i,\beta}^{(\lambda)})$ ,  $\mathbf{R}_i^{(\lambda)}(\hat{x}_{i,\beta}^{(\lambda)}; 0)$  and  $\mathbf{R}_i^{(\lambda)}(\hat{x}_{i,\beta}^{(\lambda)}; 1)$ . It can be seen that (17a) and (17b) imply

$$\begin{aligned} \mathbf{L}_i^{(m)}(y_1^n, u_1^{i-1}) &= \mathbf{R}_{i-1}^{(m)}(y_1^n, u_1^{i-2}; u_{i-1}) = \\ &= \ln \frac{\tilde{\mathbf{W}}_i^{(m),\text{ABS}+}(y_1^n, u_1^{i-1}|0)}{\tilde{\mathbf{W}}_i^{(m),\text{ABS}+}(y_1^n, u_1^{i-1}|1)} \end{aligned} \quad (19)$$

what represents the LLR for the  $i$ th message bit. In what follows we often omit the arguments and use the shortcuts  $\mathbf{L}_i^{(\lambda)} \triangleq \{\mathbf{L}_i^{(\lambda)}(\hat{x}_{i,\beta}^{(\lambda)})\}_{\beta=1}^{2^{m-\lambda}}$  and  $\mathbf{R}_i^{(\lambda)} \triangleq \{\mathbf{R}_i^{(\lambda)}(\hat{x}_{i,\beta}^{(\lambda)}; 0), \mathbf{R}_i^{(\lambda)}(\hat{x}_{i,\beta}^{(\lambda)}; 1)\}_{\beta=1}^{2^{m-\lambda}}$ .

Now let us introduce the recursive relation between  $\{\tilde{\mathbf{V}}_i^{(\lambda+1),\text{ABS}+}\}_{i=1}^{2^{\lambda+1}-1}$  and  $\{\tilde{\mathbf{V}}_j^{(\lambda),\text{ABS}+}\}_{j=1}^{2^\lambda-1}$ . For this, we define the following transforms.

**Definition 1.** Consider a channel  $V : \{0, 1\}^2 \rightarrow \mathcal{Y}$ . Then, the virtual channels

$$\begin{aligned} V^{\tilde{\nabla}}, V^{\tilde{\nabla}}, V^{\tilde{\nabla}} : \{0, 1\}^2 &\rightarrow \mathcal{Y}^2, \\ V^{\tilde{\diamond}}, V^{\tilde{\diamond}}, V^{\tilde{\diamond}} : \{0, 1\}^2 &\rightarrow \mathcal{Y}^2 \times \{0, 1\}, \\ V^{\tilde{\Delta}}, V^{\tilde{\Delta}}, V^{\tilde{\Delta}} : \{0, 1\}^2 &\rightarrow \mathcal{Y}^2 \times \{0, 1\}^2 \end{aligned}$$

are defined in the following way:

$$\begin{aligned} V^{\tilde{\nabla}}(y_1, y_2|u_1, u_2) &= \\ &= \max_{u_3, u_4 \in \{0, 1\}} V(y_1|u_1 + u_2, u_3 + u_4) V(y_2|u_2, u_4), \end{aligned} \quad (20a)$$

$$\begin{aligned} V^{\tilde{\diamond}}(y_1, y_2, u_1|u_2, u_3) &= \\ &= \max_{u_3 \in \{0, 1\}} V(y_1|u_1 + u_2, u_3 + u_4) V(y_2|u_2, u_4), \end{aligned} \quad (20b)$$

$$\begin{aligned} V^{\tilde{\Delta}}(y_1, y_2, u_1, u_2|u_3, u_4) &= \\ &= V(y_1|u_1 + u_2, u_3 + u_4) V(y_2|u_2, u_4), \end{aligned} \quad (20c)$$

$$\begin{aligned} V^{\tilde{\nabla}}(y_1, y_2|u_1, u_2) &= \\ &= \max_{u_3, u_4 \in \{0, 1\}} V(y_1|u_1 + u_3, u_2 + u_4) V(y_2|u_3, u_4), \end{aligned} \quad (21a)$$

$$\begin{aligned} V^{\tilde{\diamond}}(y_1, y_2|u_1, u_2) &= \\ &= \max_{u_3 \in \{0, 1\}} V(y_1|u_1 + u_3, u_2 + u_4) V(y_2|u_3, u_4), \end{aligned} \quad (21b)$$

$$\begin{aligned} V^{\tilde{\Delta}}(y_1, y_2|u_1, u_2) &= \\ &= V(y_1|u_1 + u_3, u_2 + u_4) V(y_2|u_3, u_4), \end{aligned} \quad (21c)$$

$$\begin{aligned} V^{\tilde{\nabla}}(y_1, y_2|u_1, u_2) &= \max_{u_3, u_4 \in \{0, 1\}} \\ &V(y_1|u_1 + u_2 + u_3, u_3 + u_4) V(y_2|u_2 + u_3, u_4), \end{aligned} \quad (22a)$$

$$\begin{aligned} V^{\tilde{\diamond}}(y_1, y_2|u_1, u_2) &= \max_{u_3 \in \{0, 1\}} \\ &V(y_1|u_1 + u_2 + u_3, u_3 + u_4) V(y_2|u_2 + u_3, u_4), \end{aligned} \quad (22b)$$

$$\begin{aligned} V^{\tilde{\Delta}}(y_1, y_2|u_1, u_2) &= \\ &= V(y_1|u_1 + u_2 + u_3, u_3 + u_4) V(y_2|u_2 + u_3, u_4). \end{aligned} \quad (22c)$$

These "approximate" channels are similar to the ones that appear after double-bit transforms  $(-)^\nabla$ ,  $(-)^\nabla$ ,  $(-)^\nabla$ , etc. from [15]. But as the transition probability we consider the probability of the most likely input vector to be transmitted. The following lemma describes the connection between the virtual channels from (16).

**Lemma 1.** Let us fix the matrices  $Q_1^{ABS+}, Q_2^{ABS+}, \dots, Q_m^{ABS+}$ ,  $m \geq 2$  according to (11) with the sets  $\mathcal{I}_S^{(m)}$  and  $\mathcal{I}_A^{(m)}$  satisfying the conditions (i)-(ii) from Section II-D. For every  $i$ :  $1 \leq i \leq n/2$  one has

(i) If  $2i \in \mathcal{I}_S^{(m)}$ , then

$$\begin{aligned}\tilde{\mathbf{V}}_{2i-1}^{(m),ABS+} &= (\tilde{\mathbf{V}}_i^{(m-1),ABS+})^{\tilde{\nabla}}, \\ \tilde{\mathbf{V}}_{2i}^{(m),ABS+} &= (\tilde{\mathbf{V}}_i^{(m-1),ABS+})^{\tilde{\Phi}}, \\ \tilde{\mathbf{V}}_{2i+1}^{(m),ABS+} &= (\tilde{\mathbf{V}}_i^{(m-1),ABS+})^{\tilde{\Lambda}}.\end{aligned}$$

(ii) If  $2i \in \mathcal{I}_A^{(m)}$ , then

$$\begin{aligned}\tilde{\mathbf{V}}_{2i-1}^{(m),ABS+} &= (\tilde{\mathbf{V}}_i^{(m-1),ABS+})^{\tilde{\nabla}}, \\ \tilde{\mathbf{V}}_{2i}^{(m),ABS+} &= (\tilde{\mathbf{V}}_i^{(m-1),ABS+})^{\tilde{\Diamond}}, \\ \tilde{\mathbf{V}}_{2i+1}^{(m),ABS+} &= (\tilde{\mathbf{V}}_i^{(m-1),ABS+})^{\tilde{\Delta}}.\end{aligned}$$

(iii) If  $2(i-1) \in \mathcal{I}_S^{(m)}$ ,  $2(i+1) \in \mathcal{I}^{(m)}$ , then

$$\tilde{\mathbf{V}}_{2i}^{(m),ABS+} = (\tilde{\mathbf{V}}_i^{(m-1),ABS+})^{\tilde{\Diamond}}.$$

(iv) If  $2(i-1) \in \mathcal{I}_S^{(m)}$ ,  $2(i+1) \notin \mathcal{I}^{(m)}$ , then

$$\begin{aligned}\tilde{\mathbf{V}}_{2i}^{(m),ABS+} &= (\tilde{\mathbf{V}}_i^{(m-1),ABS+})^{\tilde{\Diamond}}, \\ \tilde{\mathbf{V}}_{2i+1}^{(m),ABS+} &= (\tilde{\mathbf{V}}_i^{(m-1),ABS+})^{\tilde{\Delta}}.\end{aligned}$$

(v) If  $2(i-1) \notin \mathcal{I}_S^{(m)}$ ,  $2(i+1) \in \mathcal{I}^{(m)}$ , then

$$\begin{aligned}\tilde{\mathbf{V}}_{2i-1}^{(m),ABS+} &= (\tilde{\mathbf{V}}_i^{(m-1),ABS+})^{\tilde{\nabla}}, \\ \tilde{\mathbf{V}}_{2i}^{(m),ABS+} &= (\tilde{\mathbf{V}}_i^{(m-1),ABS+})^{\tilde{\Diamond}}.\end{aligned}$$

(vi) If  $2(i-1) \notin \mathcal{I}_S^{(m)}$ ,  $2i, 2(i+1) \notin \mathcal{I}^{(m)}$ , then

$$\begin{aligned}\tilde{\mathbf{V}}_{2i-1}^{(m),ABS+} &= (\tilde{\mathbf{V}}_i^{(m-1),ABS+})^{\tilde{\nabla}}, \\ \tilde{\mathbf{V}}_{2i}^{(m),ABS+} &= (\tilde{\mathbf{V}}_i^{(m-1),ABS+})^{\tilde{\Diamond}}, \\ \tilde{\mathbf{V}}_{2i+1}^{(m),ABS+} &= (\tilde{\mathbf{V}}_i^{(m-1),ABS+})^{\tilde{\Delta}}.\end{aligned}$$

We discuss the proof of this lemma in the Appendix.

Using Lemma 1, we present the formulas for a recursive calculation of the LLRs for the approximate virtual DBI subchannels. For that purpose, we consider an abstract channel  $V : \{0, 1\}^2 \rightarrow \mathcal{Y}$  and the values

$$L(y) = \ln \frac{\max_{b \in \{0, 1\}} V(y|0, b)}{\max_{b \in \{0, 1\}} V(y|1, b)}, \quad R(y; b) = \ln \frac{V(y|b, 0)}{V(y|b, 1)}. \quad (23)$$

If the values  $L(y)$  and  $R(y; b)$  are known, one can obtain the LLRs for approximate virtual subchannels from Definition 1.

**Lemma 2.** Consider a DBI channel  $V : \{0, 1\}^2 \rightarrow \mathcal{Y}$  and the functions  $L : \mathcal{Y} \rightarrow \mathbb{R}$ ,  $R : \mathcal{Y} \times \{0, 1\} \rightarrow \mathbb{R}$  from (23), some  $y_1, y_2 \in \mathcal{Y}$ ,  $u_1, u_2, b \in \{0, 1\}$  and the values

- $L^{\tilde{\nabla}}(y_1, y_2)$ ,  $R^{\tilde{\nabla}}(y_1, y_2; b)$ ,  $L^{\tilde{\nabla}}(y_1, y_2)$ ,  $R^{\tilde{\nabla}}(y_1, y_2; b)$ ,  $L^{\tilde{\nabla}}(y_1, y_2)$ ,  $R^{\tilde{\nabla}}(y_1, y_2; b)$  which are defined similarly to  $L$  and  $R$ , but  $V$  is replaced with  $V^{\tilde{\nabla}}$ ,  $V^{\tilde{\nabla}}$  or  $V^{\tilde{\nabla}}$  respectively;
- $L^{\tilde{\Diamond}}(y_1, y_2, u_1)$ ,  $R^{\tilde{\Diamond}}(y_1, y_2, u_1; b)$ ,  $L^{\tilde{\Phi}}(y_1, y_2, u_1)$ ,  $R^{\tilde{\Phi}}(y_1, y_2, u_1; b)$ ,  $L^{\tilde{\Diamond}}(y_1, y_2, u_1)$ ,  $R^{\tilde{\Diamond}}(y_1, y_2, u_1; b)$  which are defined similarly to  $L$  and  $R$ , but  $V$  is replaced with  $V^{\tilde{\Diamond}}$ ,  $V^{\tilde{\Phi}}$  or  $V^{\tilde{\Diamond}}$  respectively;

- $L^{\tilde{\Delta}}(y_1, y_2, u_1, u_2)$ ,  $R^{\tilde{\Delta}}(y_1, y_2, u_1, u_2; b)$ ,  $L^{\tilde{\Delta}}(y_1, y_2, u_1, u_2)$ ,  $R^{\tilde{\Delta}}(y_1, y_2, u_1, u_2; b)$  which are defined similarly to  $L$  and  $R$ , but  $V$  is replaced with  $V^{\tilde{\Delta}}$ ,  $V^{\tilde{\Delta}}$  or  $V^{\tilde{\Delta}}$  respectively.

For example,  $L^{\tilde{\nabla}}(y_1, y_2) = \ln \frac{\max_{b \in \{0, 1\}} V^{\tilde{\nabla}}(y_1, y_2|0, b)}{\max_{b \in \{0, 1\}} V^{\tilde{\nabla}}(y_1, y_2|1, b)}$  and

$$R^{\tilde{\Phi}}(y_1, y_2, u_1; b) = \ln \frac{V^{\tilde{\Phi}}(y_1, y_2, u_1; b)}{V^{\tilde{\Phi}}(y_1, y_2, u_1; 0)}.$$

Then, one has

$$\begin{aligned}L^{\tilde{\nabla}}(y_1, y_2) &= L^{\tilde{\nabla}}(y_1, y_2) = L^{\tilde{\nabla}}(y_1, y_2) = \\ &= f_-(L(y_1), L(y_2)),\end{aligned} \quad (24a)$$

$$\begin{aligned}L^{\tilde{\Diamond}}(y_1, y_2, u_1) &= R^{\tilde{\nabla}}(y_1, y_2; u_1) = \\ &= f_+(L(y_1), L(y_2), u_1),\end{aligned} \quad (24b)$$

$$\begin{aligned}L^{\tilde{\Phi}}(y_1, y_2, u_1) &= R^{\tilde{\nabla}}(y_1, y_2; u_1) = R^{\tilde{\Diamond}}(y_1, y_2, u_1; 1) + \\ &+ \max(0, R^{\tilde{\Phi}}(y_1, y_2, u_1; 0)) - \max(0, R^{\tilde{\Phi}}(y_1, y_2, u_1; 1)),\end{aligned} \quad (24c)$$

$$\begin{aligned}L^{\tilde{\Diamond}}(y_1, y_2, u_1) &= R^{\tilde{\nabla}}(y_1, y_2; u_1) = -R^{\tilde{\Diamond}}(y_1, y_2, u_1; 1) + \\ &+ \max(0, R^{\tilde{\Diamond}}(y_1, y_2, u_1; 0)) + \min(0, R^{\tilde{\Diamond}}(y_1, y_2, u_1; 1)),\end{aligned} \quad (24d)$$

$$\begin{aligned}L^{\tilde{\Delta}}(y_1, y_2, u_1, u_2) &= R^{\tilde{\Diamond}}(y_1, y_2, u_1; u_2) = \\ &= f_-(R(y_1; u_1 + u_2), R(y_2; u_2)),\end{aligned} \quad (24e)$$

$$\begin{aligned}L^{\tilde{\Delta}}(y_1, y_2, u_1, 0) &= R^{\tilde{\Phi}}(y_1, y_2, u_1; 0) = L^{\tilde{\Diamond}}(y_1, y_2, u_1) + \\ &+ \min(0, R^{\tilde{\Diamond}}(y_1, y_2, u_1; 0)) - \min(0, R^{\tilde{\Diamond}}(y_1, y_2, u_1; 1)),\end{aligned} \quad (24f)$$

$$\begin{aligned}L^{\tilde{\Delta}}(y_1, y_2, u_1, 1) &= R^{\tilde{\Phi}}(y_1, y_2, u_1; 1) = L^{\tilde{\Diamond}}(y_1, y_2, u_1) - \\ &- \max(0, R^{\tilde{\Diamond}}(y_1, y_2, u_1; 0)) + \max(0, R^{\tilde{\Diamond}}(y_1, y_2, u_1; 1)),\end{aligned} \quad (24g)$$

$$\begin{aligned}L^{\tilde{\Delta}}(y_1, y_2, u_1, 0) &= R^{\tilde{\Diamond}}(y_1, y_2, u_1; 0) = L^{\tilde{\Diamond}}(y_1, y_2, u_1) + \\ &+ \min(0, R^{\tilde{\Diamond}}(y_1, y_2, u_1; 0)) + \max(0, R^{\tilde{\Diamond}}(y_1, y_2, u_1; 1)),\end{aligned} \quad (24h)$$

$$\begin{aligned}L^{\tilde{\Delta}}(y_1, y_2, u_1, 1) &= R^{\tilde{\Diamond}}(y_1, y_2, u_1; 1) = -L^{\tilde{\Diamond}}(y_1, y_2, u_1) + \\ &+ \max(0, R^{\tilde{\Diamond}}(y_1, y_2, u_1; 0)) + \min(0, R^{\tilde{\Diamond}}(y_1, y_2, u_1; 1)),\end{aligned} \quad (24i)$$

$$R^{\tilde{\Delta}}(y_1, y_2, u_1, u_2; b) = f_+(R(y_1; u_1 + u_2), R(y_2; u_2), b), \quad (24j)$$

$$R^{\tilde{\Delta}}(y_1, y_2, u_1, u_2; b) = f_+(R(y_1; u_1 + u_2 + b), R(y_2; u_2 + b), b), \quad (24k)$$

$$\begin{aligned}R^{\tilde{\Delta}}(y_1, y_2, u_1, u_2; b) &= \\ &= f_+(R(y_1; u_1 + u_2 + b), R(y_1, y_2; u_2 + b); b)\end{aligned} \quad (24l)$$

with the functions  $f_+$  and  $f_-$  defined in Section II-B.

*Proof.* Note that by definition

$$V^{\tilde{\nabla}}(y_1, y_2|u_1, u_2) = \max_{u_3 \in \{0, 1\}} V^{\tilde{\nabla}}(y_1, y_2, u_1|u_2, u_3),$$

$$V^{\tilde{\nabla}}(y_1, y_2, u_1|u_2, u_3) = \max_{u_4 \in \{0, 1\}} V^{\tilde{\nabla}}(y_1, y_2, u_1, u_2|u_3, u_4), \quad (25)$$

what easily leads to  $L^{\tilde{\diamond}} = R^{\tilde{\nabla}}$ ,  $L^{\tilde{\blacklozenge}} = R^{\tilde{\nabla}}$ ,  $L^{\tilde{\diamond}} = R^{\tilde{\nabla}}$ ,  $L^{\tilde{\Delta}} = R^{\tilde{\diamond}}$ ,  $L^{\tilde{\blacklozenge}} = R^{\tilde{\blacklozenge}}$ ,  $L^{\tilde{\Delta}} = R^{\tilde{\diamond}}$  (for the simplicity, the argument lists are omitted). The proofs of (24a), (24b), (24e), (24j), (24k), (24l) are very similar; as an example we show (24b):

$$\begin{aligned} R^{\tilde{\nabla}}(y_1, y_2; u_1) &= \\ &= \ln \frac{\max_{u_3, u_4 \in \{0,1\}} V(y_1|u_1, u_3 + u_4) V(y_2|0, u_4)}{\max_{u_3, u_4 \in \{0,1\}} V(y_1|\bar{u}_1, u_3 + u_4) V(y_2|1, u_4)} \\ &= \ln \frac{\max_{u_4 \in \{0,1\}} (V(y_2|0, u_4) \max_{x \in \{0,1\}} V(y_1|u_1, x))}{\max_{u_4 \in \{0,1\}} (V(y_2|1, u_4) \max_{x \in \{0,1\}} V(y_1|\bar{u}_1, x))} \\ &= \ln \frac{(\max_{x \in \{0,1\}} V(y_1|u_1, x)) (\max_{u_4 \in \{0,1\}} V(y_2|0, u_4))}{(\max_{x \in \{0,1\}} V(y_1|\bar{u}_1, x)) (\max_{u_4 \in \{0,1\}} V(y_2|1, u_4))} \\ &= (-1)^{u_1} L(y_1) + L(y_2) = f_+(L(y_1), L(y_2), u_1) \end{aligned}$$

with the used shortcut  $\bar{u}_1 = u_1 + 1$  and relabeling  $u_3 \mapsto x = u_3 + u_4$ .

Next, we claim that the proofs of (24c) and (24f)-(24g) are analogous to that of (24d) and (24h)-(24i) respectively. Therefore, we explore only the cases (24c) and (24f). The key idea behind the proof is that

$$V^{\tilde{\blacklozenge}}(y_1, y_2, u_1|u_2, u_3) = V^{\tilde{\diamond}}(y_1, y_2, u_1|u_3, u_2). \quad (26)$$

Combining this with (25) implies  $V^{\tilde{\nabla}}(y_1, y_2|u_1, u_2) = \max_{u_3 \in \{0,1\}} V^{\tilde{\blacklozenge}}(y_1, y_2, u_1|u_2, u_3)$ . Let  $\nu(x_1, x_2) \triangleq V^{\tilde{\blacklozenge}}(y_1, y_2, u_1|x_1, x_2)$ , then

$$\begin{aligned} R^{\tilde{\nabla}}(y_1, y_2; u_1) &= \ln \frac{\max\{\nu(0,0), \nu(0,1)\}}{\max\{\nu(1,0), \nu(1,1)\}} \\ &\stackrel{a}{=} \max\{\ln \nu(0,0), \ln \nu(0,1)\} - \max\{\ln \nu(1,0), \ln \nu(1,1)\} \\ &\stackrel{b}{=} \ln \frac{\nu(0,1)}{\nu(1,1)} + \max\left\{0, \ln \frac{\nu(0,0)}{\nu(0,1)}\right\} - \max\left\{0, \ln \frac{\nu(1,0)}{\nu(1,1)}\right\} \\ &\stackrel{c}{=} R^{\tilde{\diamond}}(y_1, y_2, u_1; 1) + \max(0, R^{\tilde{\blacklozenge}}(y_1, y_2, u_1; 0)) - \\ &\quad - \max(0, R^{\tilde{\blacklozenge}}(y_1, y_2, u_1; 1)). \end{aligned}$$

The equality (a) stems from the property  $\ln \frac{a}{b} = \ln a - \ln b$  and the fact that  $\ln$  is a monotonically growing function. To get (b), we applied  $\max(a, b) = b + \max(0, a - b)$  to both max terms. The transition (c) can be easily obtained by applying to the first term (26), while in the others we simply made the substitution  $\ln \frac{\nu(x,0)}{\nu(x,1)} = R^{\tilde{\blacklozenge}}(y_1, y_2, u_1; x)$ .

To proof (24f), we use the shortcut  $\mu(x_1, x_2) \triangleq V^{\tilde{\diamond}}(y_1, y_2, u_1|x_1, x_2)$  and notice that

$$\begin{aligned} R^{\tilde{\blacklozenge}}(y_1, y_2, u_1; 0) &= \ln \frac{\nu(0,0)}{\nu(0,1)} \stackrel{(26)}{=} \ln \frac{\mu(0,0)}{\mu(1,0)} \\ &= \ln \frac{\mu(0,0)}{\mu(0,1)} + \ln \frac{\mu(0,1)}{\mu(1,1)} + \ln \frac{\mu(1,1)}{\mu(1,0)} \\ &\stackrel{d}{=} R^{\tilde{\diamond}}(y_1, y_2, u_1; 0) - R^{\tilde{\diamond}}(y_1, y_2, u_1; 0) + L^{\tilde{\diamond}}(y_1, y_2, u_1) - \\ &\quad - \max(0, R^{\tilde{\diamond}}(y_1, y_2, u_1; 0)) + \max(0, R^{\tilde{\diamond}}(y_1, y_2, u_1; 1)). \end{aligned}$$

Applying  $x - \max(0, x) = \min(0, x)$  to the last statement terminates the proof. In (d) we used the fact that

$$\ln \frac{V(y|0,1)}{V(y|1,1)} = L(y) - \max(0, R(y;0)) + \max(0, R(y;1))$$

for every DBI channel  $V$ .  $\square$

Analogously to probability-domain decoding, the LLR-based version of the algorithm computes approximate LLRs for the message bits. For this, it uses Lemmas 1 and 2. Before we discuss how to perform these operations in the proposed decoder, let us introduce some ideas that might significantly reduce the computational cost of the LLRs evaluation.

### B. Reusing intermediate values

In this section, we conjecture that naive application of the formulas from Lemma 2 in the decoder leads to performing redundant arithmetic operations. In those cases the decoder obtains exactly the same values twice. Instead of that, it might store common values (i.e. values that are needed for processing of different phases) and copy them instead of second-time evaluation.

Namely, the equalities  $L^{\tilde{\diamond}} = R^{\tilde{\nabla}}$ ,  $L^{\tilde{\blacklozenge}} = R^{\tilde{\nabla}}$ ,  $L^{\tilde{\Delta}} = R^{\tilde{\diamond}}$ ,  $L^{\tilde{\blacklozenge}} = R^{\tilde{\blacklozenge}}$ ,  $L^{\tilde{\Delta}} = R^{\tilde{\diamond}}$  agree with (19), so instead of computing  $\mathbf{L}_i^{(\lambda)}(\hat{x}_{i,\beta}^{(\lambda)})$  manually, one can reuse the value  $\mathbf{R}_{i-1}^{(\lambda)}(\hat{x}_{i-1,\beta}^{(\lambda)}; \hat{u}_{i-1,\beta}^{(\lambda)})$  with the bit  $\hat{u}_{i-1,\beta}^{(\lambda)}$  having been decoded at the  $(i-1)$ th phase.

Moreover, according to (24c), the computation of  $R^{\tilde{\nabla}}(y_1, y_2; u_1)$  requires  $R^{\tilde{\blacklozenge}}(y_1, y_2, u_1; 0)$  and  $R^{\tilde{\blacklozenge}}(y_1, y_2, u_1; 1)$  to be known. So, if  $2i \in \mathcal{I}_S^{(\lambda+1)}$ , the values  $\mathbf{R}_{2i}^{(\lambda+1)}(\hat{x}_{2i,\beta}^{(\lambda+1)}; b)$ ,  $1 \leq \beta \leq 2^{m-\lambda-1}$ ,  $b \in \{0,1\}$  are being obtained while calculating  $\mathbf{R}_{2i-1}^{(\lambda+1)}(\hat{x}_{2i-1,\beta}^{(\lambda+1)}; b)$ ,  $1 \leq \beta \leq 2^{m-\lambda-1}$ ,  $b \in \{0,1\}$  and might be simply reused. The same property holds when  $2i \in \mathcal{I}_A^{(\lambda+1)}$  (see (24d)).

The formal explanation of how these observations are injected in the decoding algorithm is given with the definition of the algorithm in Section III-D.

### C. Omitting calculations of unused LLRs

It can be noticed that the original decoding algorithm [15] of ABS+ polar codes maintains unnecessary information about transition probabilities of virtual subchannels. Namely, at the boundary layer it gets the probabilities for the  $i$ th and the  $(i+1)$ th message bits implicitly evaluated for some  $1 \leq i < n$ . Here "implicitly" means that the decoder does not store the probabilities for  $u_i$  and  $u_{i+1}$  to be 0 or 1, but the values  $\mathbb{P}(u_i = a, u_{i+1} = b)$ ,  $a, b \in \{0,1\}$ , which straightforwardly define the single-bit probabilities. However, if  $i < n-1$ , the algorithm decodes only the  $i$ th bit while the  $(i+1)$ th one is being processed only at the next phase. Instead of that, one can decode both bits at the  $i$ th phase. In this section, we suggest to generalize this idea to non-boundary layers.

In the case of LLR-domain decoding, this approach can be seen in even much simpler way. To decode the  $i$ th message bit it is sufficient to evaluate  $\mathbf{L}_i^{(m)}(y_1^n, \hat{u}_1^{i-1})$  and make the hard decision without the necessity in maintaining  $\mathbf{R}_i^{(m)}(y_1^n, \hat{u}_1^{i-1}; b)$ ,  $b \in \{0,1\}$ . Considering layers other than the  $m$ th one, we are to show that in many cases for  $0 \leq \lambda < m$ ,  $1 \leq i \leq 2^\lambda$  the decoder might estimate  $\hat{u}_i^{(\lambda)}$  without computing the values  $\mathbf{R}_i^{(\lambda)}$ .

For the convenience of the discussion, let us reformulate the SC algorithm from [15]. Here we give only high-level explanation, which are necessary for understanding of the

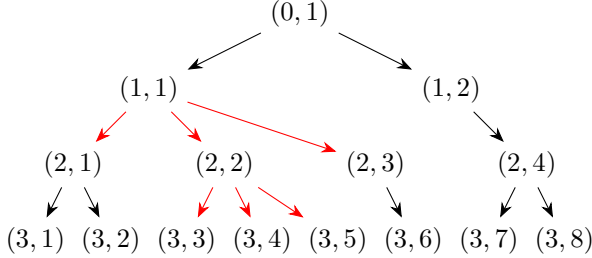


Fig. 4: The tree of the recursion in the proposed SC algorithm applied to an ABS+ polar code with  $\mathcal{I}_S^{(2)} = \emptyset$ ,  $\mathcal{I}_A^{(2)} = \{1\}$ ,  $\mathcal{I}_S^{(3)} = \{4\}$ ,  $\mathcal{I}_A^{(3)} = \emptyset$ . The algorithm performs depth-first-search starting from the root node  $(0, 1)$ ; children are being processed from left to right. We use a black edge from  $(\lambda, i)$  to  $(\lambda + 1, i')$  if  $2i \notin \mathcal{I}^{(\lambda+1)}$ . Otherwise the edge is red.

mentionned heuristic. More formal description is given in Section III-D. Unlike the original one, our version of the algorithm processes  $m + 1$  layers (numbered from zero) and  $2^\lambda$  phases at each layer  $\lambda$  (instead of  $2^\lambda - 1$ ). After the node  $(\lambda, i)$  has been processed, the algorithm has  $u_i^{(\lambda)}$  decoded. If  $\lambda = m$ , it just makes the hard decision with respect to  $\mathbf{L}_i^{(m)}$ . Otherwise, if  $2i \notin \mathcal{I}^{(\lambda+1)}$ ,  $2(i-1) \notin \mathcal{I}^{(\lambda+1)}$ , the nodes  $(\lambda + 1, 2i-1)$  and  $(\lambda + 1, 2i)$  are being recursively processed. If  $2(i-1) \in \mathcal{I}^{(\lambda+1)}$ , the algorithm processes only the node  $(\lambda + 1, 2i)$  and uses previously stored value of  $\hat{u}_{2i-1}^{(\lambda+1)}$ . If  $2i \in \mathcal{I}^{(\lambda+1)}$ , the algorithm additionally processes the node  $(\lambda + 1, 2i+1)$ . If  $2i \in \mathcal{I}_S^{(\lambda+1)}$ ,  $\hat{u}_{2i}^{(\lambda+1)}$  is being stored and  $\hat{u}_i^{(\lambda)}$  is calculated with accordance to (13c). If  $2i \in \mathcal{I}_A^{(\lambda+1)}$ ,  $\hat{u}_{2i+1}^{(\lambda+1)}$  is being stored and  $\hat{u}_i^{(\lambda)}$  is calculated with accordance to (13d). As the input for processing of the node  $(\lambda, i)$  the algorithm receives  $\mathbf{L}_i^{(\lambda)}, \mathbf{R}_i^{(\lambda)}$  if  $i < 2^\lambda$  and only  $\mathbf{L}_i^{(\lambda)}$  if  $i = 2^\lambda$ . In the case  $i < 2^\lambda$ , the decoder uses Lemmas 1 and 2 to calculate  $\mathbf{L}_i^{(\lambda)}$  and  $\mathbf{R}_i^{(\lambda)}$ . If  $i = 2^\lambda$ , the decoder reuses  $\mathbf{R}_{i-1}^{(\lambda)}$ :  $\mathbf{L}_i^{(\lambda)}(\hat{x}_{i,\beta}) = \mathbf{R}_{i-1}^{(\lambda)}(\hat{x}_{i,\beta}; \hat{u}_{i-1,\beta}^{(\lambda)}), 1 \leq \beta \leq 2^{m-\lambda}$ . The initial values in this recursive procedure are  $\mathbf{L}_1^{(0)}(y_\beta) = \ln \frac{W(y_\beta|0)}{W(y_\beta|1)}$ ,  $1 \leq \beta \leq n$ . Finally, since  $2^{\lambda+1}$  never belongs to  $\mathcal{I}^{(\lambda+1)}$ , for computing  $\mathbf{L}_{2^{\lambda+1}}^{(\lambda+1)}$  it is sufficient to know only  $\mathbf{L}_{2^\lambda}^{(\lambda)}$  and  $\hat{u}_{2^\lambda-1}^{(\lambda+1)}$  (see (24b)). An example of the recursion tree in the reformulated SC decoder is given in Fig. 4.

Note that for all  $0 \leq \lambda \leq m$  the node  $(\lambda, i = 2^\lambda)$  can be processed if only  $\mathbf{L}_i^{(\lambda)}$  is known. But there may be some other nodes requiring only such single-bit LLRs for their processing. So, let us investigate the cases when  $\mathbf{R}_i^{(\lambda)}$  is indeed needed for decoding of  $u_i^{(\lambda)}$ . The key observation is that if  $2i \notin \mathcal{I}^{(\lambda+1)}$ , according to (24a) and (24b), one can obtain  $\mathbf{L}_{2i-1}^{(\lambda+1)}, \mathbf{R}_{2i-1}^{(\lambda+1)}$  and  $\mathbf{L}_{2i}^{(\lambda)}$  by taking into account only the values  $\mathbf{L}_i^{(\lambda)}$  (and also  $u_{2i-1}^{(\lambda)}$  which is being decoded at the  $(2i-1)$ th phase of the layer  $\lambda + 1$ ). Note that in this case  $\hat{u}_{2i+1}^{(\lambda+1)}$  is not required for decoding of  $u_i^{(\lambda)}$  (see (13a)). However, the "right" component vector in the decomposition of  $u_{2i}^{(\lambda+1)}$  may require  $\mathbf{R}_{2i}^{(\lambda+1)}$  in order to be decoded. To calculate these LLRs, the decoder must have  $\mathbf{R}_i^{(\lambda)}$  computed (see (24j)). So, for  $1 \leq i < 2^\lambda$  the

---

**Algorithm 1: SC( $y_1, \dots, y_n$ )**


---

```

1 for  $\beta \in \{1, 2, \dots, n\}$  do
2   |  $\mathbf{L}[0, \beta] \leftarrow \ln \frac{W(y_\beta|0)}{W(y_\beta|1)}$ ;
3   | DecodeNode( $0, 1$ );
4 for  $\beta \in \{1, 2, \dots, n\}$  do
5   |  $\hat{c}_\beta \leftarrow \mathbf{B}[0, \beta]$ ;
6 return  $\hat{c}_1^n$ ;

```

---

algorithm does not use  $\mathbf{R}_i^{(\lambda)}$  for processing of the node  $(\lambda, i)$  if both conditions hold:

- 1)  $2i \notin \mathcal{I}^{(\lambda+1)}$ ;
- 2)  $\lambda = m$  or the algorithm does not use  $\mathbf{R}_{2i}^{(\lambda+1)}$  in order to process the node  $(\lambda + 1, 2i)$ .

Let us give a more precise explanation of those conditions. While processing of the node  $(\lambda, i)$  the decoder often estimates not only the vector  $u_i^{(\lambda)}$ , but also some component vectors in the decomposition of  $u_i^{(\lambda)}$ . Namely, if  $2i \in \mathcal{I}^{(\lambda+1)}$ , it is necessary to decode all vectors  $u_{2i-1}^{(\lambda+1)}, u_{2i}^{(\lambda+1)}$  and  $u_{2i+1}^{(\lambda+1)}$ , although their mapping to  $u_i^{(\lambda)}$  is not bijective. Then, one of the decoded vectors is being stored, because it is needed for processing of the node  $(\lambda, i + 1)$ . Moreover, even if  $2i \notin \mathcal{I}^{(\lambda+1)}$ , after processing of the node  $(\lambda, i)$ , the vector  $u_{i+1}^{(\lambda)}$  may be "partially" decoded. This takes place when in the recursion tree some child  $(\lambda' < m, i')$  of  $(\lambda, i)$  from its rightmost branch satisfies  $2i' \in \mathcal{I}^{(\lambda'+1)}$ . So, both conditions (1) and (2) hold iff all the edges on the rightmost path from  $(\lambda, i)$  to a leaf node have the form  $(\lambda', i') \rightarrow (\lambda' + 1, 2i')$ . In what follows we call such nodes  $(\lambda, i)$  *right-separated*, because at every layer  $\lambda' > \lambda$  the rightmost node in the subtree of  $(\lambda, i)$  precedes the leftmost node in the subtree of  $(\lambda, i+1)$ <sup>1</sup>. Note that after the node  $(\lambda, i)$  has been processed in the SC decoder, it has the message bits  $u_1, u_2, \dots, u_j$  estimated where  $(m, j)$  is the rightmost leaf node in the subtree of  $(\lambda, i)$ . Therefore, if  $(\lambda, i)$  is not right-separated, there are some message bits which are being decoded at the current phase and whose values restrict the set of all possible values of  $u_{i+1}^{(\lambda)}$ . In this cases we indeed need to take into account some information about bits of  $u_{i+1}^{(\lambda)}$ , what is represented by  $\mathbf{R}_i^{(\lambda)}$ .

#### D. The proposed LLR-based SC decoding algorithm

Let us move to the formal definition of the proposed SC decoding algorithm which is announced in Sections III-B and III-C. The main endpoint is presented in Algorithm 1, where the recursive procedure DecodeNode from Algorithm 2 is called to process the root node. The function DecodeNode( $\lambda, i$ ) processes the node  $(\lambda, i)$  in the way discussed above. To explore it precisely, consider the underlying data structures.

- 2-dimensional array  $\mathbf{B}$  of decoded bits. For  $0 \leq \lambda \leq m$ ,  $1 \leq i \leq 2^\lambda$ ,  $1 \leq \beta \leq 2^{m-\lambda}$  after the function

<sup>1</sup> $(\lambda, 2^\lambda)$  is the rightmost node at the layer and we also consider it as right-separated

---

**Algorithm 2:** DecodeNode( $\lambda, i$ )

---

```

1 if  $\lambda = m$  then
2   if  $i \notin \mathcal{F}$  and  $\mathbb{L}[m, 1] < 0$  then
3      $\mathbb{B}[m, 1] \leftarrow 1$ ;
4   else
5      $\mathbb{B}[m, 1] \leftarrow 0$ ;
6   return;
7  $N \leftarrow 2^{m-\lambda}$ ;
8 if  $2(i-1) \notin \mathcal{I}^{(\lambda+1)}$  then
9   for  $\beta \in \{1, 2, \dots, N/2\}$  do
10    | CalculateLLRs_LeftBranch( $\lambda, i, \beta$ );
11    DecodeNode( $\lambda + 1, 2i - 1$ );
12    for  $\beta \in \{1, 2, \dots, N/2\}$  do
13      |  $\mathbb{B}[\lambda, \beta] \leftarrow \mathbb{B}[\lambda + 1, \beta]$ ;
14 else
15   for  $\beta \in \{1, 2, \dots, N/2\}$  do
16     |  $\mathbb{B}[\lambda, \beta] \leftarrow \mathbb{H}[\lambda, \beta]$ ;
17 for  $\beta \in \{1, 2, \dots, N/2\}$  do
18   | CalculateLLRs_MiddleBranch( $\lambda, i, \beta$ );
19 DecodeNode( $\lambda + 1, 2i$ );
20 if  $2i \notin \mathcal{I}^{(\lambda+1)}$  then
21   for  $\beta \in \{1, 2, \dots, N/2\}$  do
22     |  $\beta' \leftarrow \beta + N/2$ ,  $r_1 \leftarrow \mathbb{B}[\lambda, \beta]$ ,  $r_2 \leftarrow \mathbb{B}[\lambda + 1, \beta]$ ;
23     |  $\mathbb{B}[\lambda, \beta] \leftarrow r_1 + r_2$ ,  $\mathbb{B}[\lambda, \beta'] \leftarrow r_2$ ;
24 else
25   for  $\beta \in \{1, 2, \dots, N/2\}$  do
26     |  $\mathbb{B}[\lambda, \beta + N/2] \leftarrow \mathbb{B}[\lambda + 1, \beta]$ ;
27   for  $\beta \in \{1, 2, \dots, N/2\}$  do
28     | CalculateLLRs_RightBranch( $\lambda, i, \beta$ );
29 DecodeNode( $\lambda + 1, 2i + 1$ );
30 for  $\beta \in \{1, 2, \dots, N/2\}$  do
31   |  $\beta' \leftarrow \beta + N/2$ ,  $r_1 \leftarrow \mathbb{B}[\lambda, \beta]$ ,  $r_2 \leftarrow \mathbb{B}[\lambda, \beta']$ ,  $r_3 \leftarrow \mathbb{B}[\lambda + 1, \beta]$ ;
32   if  $2i \in \mathcal{I}_S^{(\lambda+1)}$  then
33     |  $\mathbb{B}[\lambda, \beta] \leftarrow r_1 + r_3$ ,  $\mathbb{B}[\lambda, \beta'] \leftarrow r_3$ ;
34     |  $\mathbb{H}[\lambda, \beta] \leftarrow r_2$ ;
35   if  $2i \in \mathcal{I}_A^{(\lambda+1)}$  then
36     |  $\mathbb{B}[\lambda, \beta] \leftarrow r_1 + r_2 + r_3$ ,  $\mathbb{B}[\lambda, \beta'] \leftarrow r_2 + r_3$ ;
37     |  $\mathbb{H}[\lambda, \beta] \leftarrow r_3$ ;

```

---

DecodeNode( $\lambda, i$ ) has returned,  $\mathbb{B}[\lambda, \beta]$  stores the estimated bit  $\hat{u}_{i,\beta}^{(\lambda)}$ .

- 2-dimensional array  $\mathbb{H}$  of decoded bits that are needed for processing of a next phase. For  $0 \leq \lambda < m$ ,  $1 \leq i \leq 2^\lambda$ ,  $1 \leq \beta \leq 2^{m-\lambda-1}$  after the function DecodeNode( $\lambda, i$ ) has returned,  $\mathbb{H}[\lambda, \beta]$  stores either  $\hat{u}_{2i,\beta}^{(\lambda+1)}$  if  $2i \in \mathcal{I}_S^{(\lambda+1)}$  or  $\hat{u}_{2i+1,\beta}^{(\lambda+1)}$  if  $2i \in \mathcal{I}_A^{(\lambda+1)}$ .
- 2-dimensional array  $\mathbb{L}$  of real numbers representing  $\mathbb{L}_i^{(\lambda)}$ . For  $0 \leq \lambda \leq m$ ,  $1 \leq i \leq 2^\lambda$ ,  $1 \leq \beta \leq 2^{m-\lambda}$  after the function DecodeNode( $\lambda, i$ ) has been called,  $\mathbb{L}[\lambda, \beta]$  stores  $\mathbb{L}_i^{(\lambda)}(\hat{x}_{i,\beta}^{(\lambda)})$ .
- 2-dimensional array  $\mathbb{R}$  of pairs of real numbers representing  $\mathbb{R}_i^{(\lambda)}$ . Consider  $0 \leq \lambda \leq m$ ,  $1 \leq i \leq 2^\lambda$ ,  $1 \leq \beta \leq 2^{m-\lambda}$ ,  $b \in \{0, 1\}$  such that the node  $(\lambda, i)$  is not right-separated. After the function DecodeNode( $\lambda, i$ ) has been

called,  $\mathbb{R}[\lambda, \beta][b]$  stores  $\mathbb{R}_i^{(\lambda)}(\hat{x}_{i,\beta}^{(\lambda+1)}; b)$ .

- 2-dimensional array  $\mathbb{M}$  of quadruples of real numbers representing the intermediate values that can be reused while LLR computations (see Section III-B). Consider  $0 \leq \lambda < m$ ,  $1 \leq i \leq 2^\lambda$ ,  $1 \leq \beta \leq 2^{m-\lambda-1}$  such that  $2i \in \mathcal{I}^{(\lambda+1)}$ . If the node  $(\lambda + 1, 2i - 1)$  is not right-separated, after  $\mathbb{R}_{2i-1}^{(\lambda+1)}(\hat{x}_{2i-1,\beta}^{(\lambda+1)}; a)$ ,  $a \in \{0, 1\}$  has been computed,  $\mathbb{M}[\lambda, \beta][a, b]$ ,  $b \in \{0, 1\}$  stores  $\mathbb{R}_{2i}^{(\lambda+1)}(\hat{x}_{2i,\beta}^{(\lambda+1)}; b)$  with assumption  $\hat{u}_{2i,\beta}^{(\lambda+1)} = a$ . If the node  $(\lambda + 1, 2i - 1)$  is right-separated but  $(\lambda + 1, 2i)$  is not, after  $\mathbb{L}_{2i}^{(\lambda+1)}(\hat{x}_{2i,\beta})$  has been computed,  $\mathbb{M}[\lambda, \beta][\hat{u}_{2i,\beta}^{(\lambda+1)}, b]$ ,  $b \in \{0, 1\}$  stores  $\mathbb{R}_{2i}^{(\lambda+1)}(\hat{x}_{2i,\beta}^{(\lambda+1)}; b)$ .

We also use the shortcut  $\mathbb{A}[\lambda, *]$  to denote the array  $[\mathbb{A}[\lambda, 1], \mathbb{A}[\lambda, 2], \dots]$  for any 2-dimensional array  $\mathbb{A}$ .

In the case  $\lambda = m$  it is sufficient to make the hard decision with respect to the sign of LLR:

$$\hat{u}_i = \begin{cases} 1, & i \notin \mathcal{F} \text{ and } \mathbb{L}_i^{(m)}(y_1^n, \hat{u}_1^{i-1}) < 0, \\ 0, & \text{otherwise.} \end{cases} \quad (27)$$

Otherwise, the nodes of the layer  $\lambda + 1$  are being processed. In lines 10, 18 and 28 of the Algorithm 2 we perform the computation of the LLRs for the virtual channels  $\tilde{\mathbf{V}}_{2i-1}^{(\lambda+1), \text{ABS}^+}$ ,  $\tilde{\mathbf{V}}_{2i}^{(\lambda+1), \text{ABS}^+}$  and  $\tilde{\mathbf{V}}_{2i+1}^{(\lambda+1), \text{ABS}^+}$  respectively. Then, after the necessary nodes of the next layer have been processed, the resulting vector  $\hat{u}_i^{(\lambda)}$  is calculated. Namely, if  $2i \notin \mathcal{I}^{(\lambda+1)}$ , in line 23 one of the formulas (13a)-(13b) is used; if  $2i \in \mathcal{I}_S^{(\lambda+1)}$ , in line 33 the formula (13c) is used, and finally if  $2i \in \mathcal{I}_A^{(\lambda+1)}$ , we use the formula (13d) in line 36. Moreover, if  $2i \in \mathcal{I}^{(\lambda+1)}$ , the array  $\mathbb{H}$  is being updated (see lines 34 and 37). The stored value will be read in line 16 while execution DecodeNode( $\lambda, i + 1$ ).

In essence, the differences between our function DecodeNode( $\lambda, i$ ) and the recursive procedure for decoding of ABS+ polar codes from [15] are very minor. Firstly, our function accepts pairs  $(\lambda, i)$  such that  $0 \leq \lambda \leq m$ ,  $1 \leq i \leq 2^\lambda$  (instead of  $1 \leq \lambda \leq m$ ,  $1 \leq i \leq 2^{\lambda-1}$ ). Secondly, in the case  $i = 2^\lambda - 1$  we do not decode  $u_{i+1}^{(\lambda)}$  while processing the node  $(\lambda, i)$ . Instead, there are the additional node  $(\lambda, 2^\lambda)$  in the recursion tree. And finally, the underlying arithmetic operations performed in the LLR-domain.

Now consider the Algorithms 3, 4 and 5 representing evaluation of the LLRs. In all these functions we assign the arrays  $\mathbb{L}[\lambda+1, *]$  and  $\mathbb{R}[\lambda+1, *]$  in order to have the necessary LLRs computed before processing of nodes  $(\lambda + 1, 2i - 1)$ ,  $(\lambda + 1, 2i)$  and  $(\lambda + 1, 2i + 1)$  respectively. The array  $\mathbb{R}[\lambda+1, *]$  is being assigned if and only if the "current" node (i.e.  $(\lambda + 1, 2i - 1)$ ,  $(\lambda + 1, 2i)$  and  $(\lambda + 1, 2i + 1)$  for Algorithms 3, 4 and 5 respectively) is not right-separated. Therefore, if the "preceding" node (i.e.  $(\lambda + 1, 2i - 2)$ ,  $(\lambda + 1, 2i - 1)$  and  $(\lambda + 1, 2i)$  for Algorithms 3, 4 and 5 respectively) is not right-separated, at the beginning of the function  $\mathbb{R}[\lambda+1, *]$  already includes the desired values for  $\mathbb{L}[\lambda+1, *]$ , so it is sufficient to copy the entries corresponding to the last decoded bit. Otherwise, the entries of  $\mathbb{L}[\lambda+1, *]$  are computed manually.

**Algorithm 3:** CalculateLLRs\_LeftBranch( $\lambda, i, \beta$ )

---

```

1  $\beta' \leftarrow \beta + 2^{m-\lambda-1};$ 
  // Calculate  $\mathbf{L}_{2i-1}^{(\lambda+1)}$ 
2 if  $i > 1$  and  $(\lambda + 1, 2i - 2)$  is not right-separated then
3    $r_0 \leftarrow \mathbf{B}[\lambda + 1, \beta] \quad // \quad r_0 = \hat{u}_{2i-2, \beta}^{(\lambda+1)}$ 
4    $\mathbf{L}[\lambda, \beta] \leftarrow \mathbf{R}[\lambda, \beta][r_0];$ 
5 else
6    $\mathbf{L}[\lambda + 1, \beta] \leftarrow f_-(\mathbf{L}[\lambda, \beta], \mathbf{L}[\lambda, \beta']) \quad // \quad \text{see (24a)}$ 
7 if  $(\lambda + 1, 2i - 1)$  is not right-separated then
8   // Calculate  $\mathbf{R}_{2i-1}^{(\lambda+1)}$ 
9   for  $b \in \{0, 1\}$  do
10  if  $2i \notin \mathcal{I}^{(\lambda+1)}$  then
11     $\mathbf{R}[\lambda + 1, \beta][b] \leftarrow f_+(\mathbf{L}[\lambda, \beta], \mathbf{L}[\lambda, \beta'], b);$ 
12  else
13     $R_0 \leftarrow f_-(\mathbf{R}[\lambda, \beta][b], \mathbf{R}[\lambda, \beta'][0]);$ 
14     $R_1 \leftarrow f_-(\mathbf{R}[\lambda, \beta][b + 1], \mathbf{R}[\lambda, \beta'][1]);$ 
15     $L \leftarrow f_+(\mathbf{L}[\lambda, \beta], \mathbf{L}[\lambda, \beta'], b);$ 
16    if  $2i \in \mathcal{I}_S^{(\lambda+1)}$  then
17       $\mathbf{M}[\lambda, \beta][b, 0] \leftarrow$ 
18         $L + \min\{0, R_0\} - \min\{0, R_1\}$ 
19        // see (24f)
20       $\mathbf{M}[\lambda, \beta][b, 1] \leftarrow$ 
21         $L - \max\{0, R_0\} + \max\{0, R_1\}$ 
22        // see (24g)
23       $\mathbf{R}[\lambda, \beta][b] \leftarrow$ 
24         $R_1 + \max\{0, \mathbf{M}[\lambda, \beta][b, 0]\} -$ 
25         $\max\{0, \mathbf{M}[\lambda, \beta][b, 1]\} \quad // \quad \text{see}$ 
26        (24c)
27      if  $2i \in \mathcal{I}_A^{(\lambda+1)}$  then
28         $\mathbf{M}[\lambda, \beta][b, 0] \leftarrow$ 
29           $L + \min\{0, R_0\} + \min\{0, R_1\}$ 
30          // see (24h)
31         $\mathbf{M}[\lambda, \beta][b, 1] \leftarrow$ 
32           $-L + \max\{0, R_0\} + \max\{0, R_1\}$ 
33          // see (24i)
34       $\mathbf{R}[\lambda, \beta][b] \leftarrow$ 
35         $-R_1 + \max\{0, \mathbf{M}[\lambda, \beta][b, 0]\} +$ 
36         $\min\{0, \mathbf{M}[\lambda, \beta][b, 1]\} \quad // \quad \text{see}$ 
37        (24d)

```

---

**Algorithm 4:** CalculateLLRs\_MiddleBranch( $\lambda, i, \beta$ )

---

```

1  $\beta' \leftarrow \beta + 2^{m-\lambda-1}, r_1 \leftarrow \mathbf{B}[\lambda + 1, \beta];$ 
2 if  $(\lambda + 1, 2i - 1)$  is right-separated and  $2i \in \mathcal{I}^{(\lambda+1)}$  then
3   // Need to calculate  $\mathbf{R}_{2i}^{(\lambda+1)}$ 
4    $L \leftarrow f_+(\mathbf{L}[\lambda, \beta], \mathbf{L}[\lambda, \beta'], r_1);$ 
5    $R_0 \leftarrow f_-(\mathbf{R}[\lambda, \beta][r_1], \mathbf{R}[\lambda, \beta'][0]);$ 
6    $R_1 \leftarrow f_-(\mathbf{R}[\lambda, \beta][r_1 + 1], \mathbf{R}[\lambda, \beta'][1]);$ 
7   if  $2i \in \mathcal{I}_S^{(\lambda+1)}$  then
8      $\mathbf{M}[\lambda, \beta][r_1, 0] \leftarrow L + \min\{0, R_0\} - \min\{0, R_1\}$ 
8     // see (24f)
9      $\mathbf{M}[\lambda, \beta][r_1, 1] \leftarrow L - \max\{0, R_0\} + \max\{0, R_1\}$ 
9     // see (24g)
10    if  $2i \in \mathcal{I}_A^{(\lambda+1)}$  then
11       $\mathbf{M}[\lambda, \beta][r_1, 0] \leftarrow L + \min\{0, R_0\} + \max\{0, R_1\}$ 
11      // see (24h)
12       $\mathbf{M}[\lambda, \beta][r_1, 1] \leftarrow -L + \max\{0, R_0\} + \min\{0, R_1\}$ 
12      // see (24i)
13      // Calculate  $\mathbf{L}_{2i}^{(\lambda+1)}$ 
14      if  $(\lambda + 1, 2i - 1)$  is not right-separated then
15         $\mathbf{L}[\lambda + 1, \beta] \leftarrow \mathbf{R}[\lambda + 1, \beta][r_1];$ 
16      else
17        if  $2i \notin \mathcal{I}^{(\lambda+1)}$  then
18           $\mathbf{L}[\lambda + 1, \beta] \leftarrow f_+(\mathbf{L}[\lambda, \beta], \mathbf{L}[\lambda, \beta'], r_1);$ 
19        if  $2i \in \mathcal{I}_S^{(\lambda+1)}$  then
20           $\mathbf{L}[\lambda + 1, \beta] \leftarrow R_1 + \max\{0, \mathbf{M}[\lambda, \beta][r_1, 0]\} -$ 
21           $\max\{0, \mathbf{M}[\lambda, \beta][r_1, 1]\} \quad // \quad \text{see (24c)}$ 
22        if  $2i \in \mathcal{I}_A^{(\lambda+1)}$  then
23           $\mathbf{L}[\lambda + 1, \beta] \leftarrow -R_1 + \max\{0, \mathbf{M}[\lambda, \beta][r_1, 0]\} +$ 
24           $\min\{0, \mathbf{M}[\lambda, \beta][r_1, 1]\} \quad // \quad \text{see (24d)}$ 
25      if  $(\lambda + 1, 2i)$  is not right-separated then
26        // Calculate  $\mathbf{R}_{2i}^{(\lambda+1)}$ 
27        if  $2i \notin \mathcal{I}^{(\lambda+1)}$  then
28          // see (24e)
29         $\mathbf{R}[\lambda + 1, \beta][0] \leftarrow f_-(\mathbf{R}[\lambda, \beta][r_1], \mathbf{R}[\lambda, \beta'][0]);$ 
30         $\mathbf{R}[\lambda + 1, \beta][1] \leftarrow f_-(\mathbf{R}[\lambda, \beta][r_1 + 1], \mathbf{R}[\lambda, \beta'][1]);$ 
31      else
32         $\mathbf{R}[\lambda + 1, \beta][0] \leftarrow \mathbf{M}[\lambda, \beta][r_1, 0];$ 
33         $\mathbf{R}[\lambda + 1, \beta][1] \leftarrow \mathbf{M}[\lambda, \beta][r_1, 1];$ 

```

---

**E. SCL decoding in the LLR domain**

The SCL decoder maintains the arrays  $\mathbf{B}, \mathbf{H}, \mathbf{L}, \mathbf{R}, \mathbf{M}$  for every active path using the data structures from [2] or [14]. At the  $i$ th phase of the boundary layer the path metrics are being updated with respect to (10) with  $\alpha = \mathbf{L}_i^{(m)}(y_1^n, \hat{u}_1^{i-1})$ .

The non-trivial detail is that in line 3 of Algorithm 3 the entries of  $\mathbf{B}[\lambda + 1, *]$  may refer to another path. To address this issue, one can store an additional array for every path where the decoder saves  $\mathbf{R}_i^{(\lambda)}(\hat{x}_{i, \beta}^{(\lambda)}; \hat{u}_{i, \beta}^{(\lambda)})$ ,  $1 \leq \beta \leq 2^{m-\lambda}$  right after the vector  $\hat{u}_i^{(\lambda)}$  has been obtained. And instead of line 4 in Algorithm 3 the decoder reads these LLRs.

**Proposition 1.** *The presented SCL decoder of ABS+ polar codes with the infinite list size performs ML decoding.*

**Algorithm 5:** CalculateLLRs\_RightBranch( $\lambda, i, \beta$ )

---

```

1  $\beta' \leftarrow \beta + 2^{m-\lambda-1}, r_1 \leftarrow \mathbf{B}[\lambda, \beta], r_2 \leftarrow \mathbf{B}[\lambda, \beta'];$ 
2  $\mathbf{L}[\lambda + 1, \beta] \leftarrow \mathbf{M}[\lambda, \beta][r_1, r_2];$ 
3 if  $(\lambda + 1, 2i + 1)$  is not right-separated then
4   // Calculate  $\mathbf{R}_{2i+1}^{(\lambda+1)}$ 
5   for  $b \in \{0, 1\}$  do
6     if  $2i \in \mathcal{I}_S^{(\lambda+1)}$  then
7        $\mathbf{R}[\lambda + 1, \beta][b] \leftarrow$ 
7        $f_+(\mathbf{R}[\lambda, \beta][r_1 + b], \mathbf{R}[\lambda, \beta'][b], r_2)$ 
7       // see (24k)
8     if  $2i \in \mathcal{I}_A^{(\lambda+1)}$  then
9        $\mathbf{R}[\lambda + 1, \beta][b] \leftarrow$ 
9        $f_+(\mathbf{R}[\lambda, \beta][r_1 + r_2 + b], \mathbf{R}[\lambda, \beta'][r_2 + b], b)$ 
9       // see (24l)

```

---

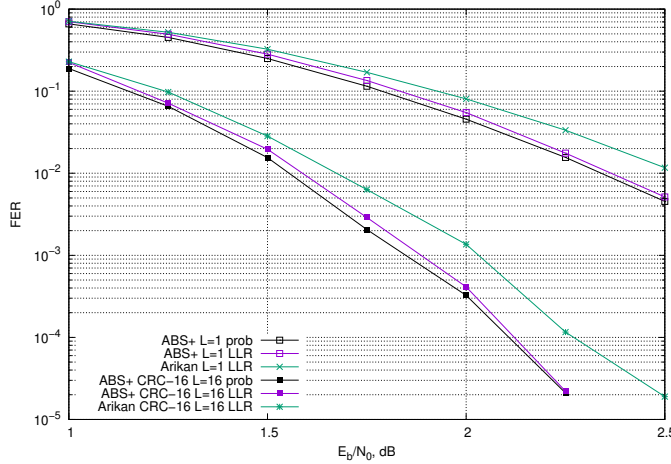


Fig. 5: Comparison of (1024, 512) polar codes.

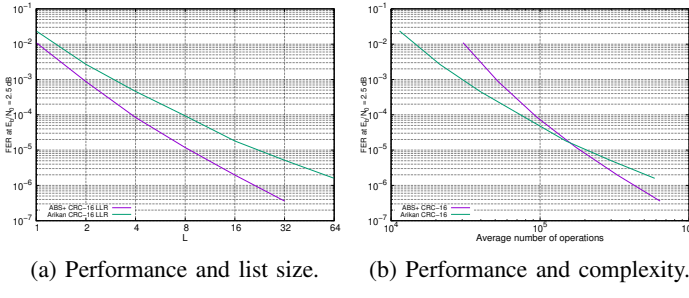


Fig. 6: Comparison of (1024, 512) codes under SCL decoding with varied list size.

#### IV. NUMERIC RESULTS

In this section we present some simulation results in the case of AWGN channel and BPSK modulation.

In Fig. 5 (1024, 512) Arikan and ABS+ polar codes are compared under SC and CRC-aided SCL decoding. The codes were constructed for AWGN channel with  $E_b/N_0 = 2$  dB. In both cases the proposed LLR-based decoder of ABS+ polar codes outperforms that of the standard ones providing the the frame error rate (FER) gain up to 0.25 dB which increases with growing of  $E_b/N_0$ . Furthermore, the proposed decoder is compared against the similar probability-domain SCL ABS+ decoder. We observe a small performance loss that does not exceed 0.05 dB.

Fig. 6a represents the dependency between the list size  $L$  and FER performance at the fixed  $E_b/N_0 = 2.5$  dB. It can be noticed that the SCL decoder of ABS+ polar codes requires much smaller list size than that of Arikans polar codes in order to get the same performance. Finally, in Fig. 6b we investigate the dependency between FER and the number of additions and comparisons of LLRs in the decoder. For  $L \geq 12$  the ABS+ SCL decoder demonstrates better FER than the standard SCL, which uses the same number of arithmetic operations.

#### V. CONCLUSIONS

In this paper, a low-complexity LLR-based version of the SCL decoder of ABS+ polar codes is discovered. This makes ABS+ polar codes applicable for a practical usage.

We introduced the approximation of LLRs of virtual sub-channels stemming from the ABS+ encoding process. These LLRs, used in the proposed decoder, correspond to most likely continuations of a decoded message prefix. Therefore, our decoder provably asymptotically achieves ML. Meanwhile, for a finite list size, the loss to the similar probability-domain SCL decoder is negligibly small.

The presented min-sum approximation can be used to generalize other polar decoding approaches (e.g. sequential decoding [5]) to ABS+ polar codes. Moreover, one can apply the techniques of fast SC and SCL [19], [17] decoding to the proposed decoder.

#### APPENDIX

##### A. Proof of Lemma 1

The proof is very similar to that of Lemma 2 from [14] and Lemma 3 from [15]. So, we restrict the strict part of the proof to the case (vi) while the others can be proven by generalizing this proof in the straightforward way.

Let us introduce some additional notations. We denote the  $l \times l$  identity matrix as  $I_l$ . For random variables  $\xi$  and  $\eta$  whose values belong to the sets  $\mathbb{X}$  and  $\mathbb{Y}$  respectively and for  $x \in \mathbb{X}$ ,  $y \in \mathbb{Y}$  we use  $\mathbb{P}_{\xi|\eta}(x|y)$  to denote the conditional probability density of the distribution  $\xi$  in the point  $x$  with the condition  $\eta = y$ .

As in [14, Proof of Lemma 1], consider a random vector  $U_1^n$ , where  $U_j$  is the Bernoulli-distributed value with  $\mathbb{P}_{U_j}(0) = \mathbb{P}_{U_j}(1) = 1/2$  and all  $U_j$ 's are independent. Next, let  $X_1^n = U_1^n G_m^{\text{ABS+}}$  and  $Y_j$  is the random value corresponding to the output of  $W$  if  $X_j$  is given as the input. It is obvious that  $W(y|x) = \mathbb{P}_{Y_j|X_j}(y|x)$ ,  $y \in \mathbb{Y}$ ,  $x \in \{0, 1\}$  and therefore

$$\mathbf{W}^{(m),\text{ABS+}}(y_1^n|u_1^n) = \mathbb{P}_{Y_1^n|U_1^n}(y_1^n|u_1^n) \quad (28)$$

for every  $y_1^n \in \mathbb{Y}^n$ ,  $u_1^n \in \{0, 1\}^n$ .

Let  $\tilde{U}_1^n = U_1^n Q_m^{\text{ABS+}}(I_{n/2} \otimes F)$ . Saying informally,  $\tilde{U}_1^n$  represents the result of passing  $U_1^n$  through the leftmost layer of the encoding circuit in terms of Fig. 2. Since  $G_m^{\text{ABS+}} = Q_m^{\text{ABS+}}(G_{m-1}^{\text{ABS+}} \otimes F) = Q_m^{\text{ABS+}}(I_{n/2} \otimes F)(G_{m-1}^{\text{ABS+}} \otimes I_2)$ , one has  $X_1^n = \tilde{U}_1^n(G_{m-1}^{\text{ABS+}} \otimes I_2)$  and hence  $X_{1,o}^n = \tilde{U}_{1,o}^n G_{m-1}^{\text{ABS+}}$  and  $X_{1,e}^n = \tilde{U}_{1,e}^n G_{m-1}^{\text{ABS+}}$ . Therefore, the random vectors  $(Y_{1,o}^n|\tilde{U}_{1,o})$  and  $(Y_{1,e}^n|\tilde{U}_{1,e})$  are independent. This implies

$$\begin{aligned} \tilde{\mathbf{V}}_{2i-1}^{(m),\text{ABS+}}(y_1^n, u_1^{2i-2}|u_{2i-1}, u_{2i}) &= \\ &= \max_{u_{2i+1}^n} \mathbf{W}^{(m),\text{ABS+}}(y_1^n|u_1^n) = \max_{u_{2i+1}^n} \mathbb{P}_{Y_1^n|U_1^n}(y_1^n|u_1^n) \\ &\stackrel{(a)}{=} \max_{u_{2i+1}^n} \mathbb{P}_{Y_{1,o}^n|\tilde{U}_{1,o}^n}(y_{1,o}^n|\tilde{u}_{1,o}^n) \mathbb{P}_{Y_{1,e}^n|\tilde{U}_{1,e}^n}(y_{1,e}^n|\tilde{u}_{1,e}^n) \\ &\stackrel{(b)}{=} \max_{u_{2i+1}^n} \mathbf{W}^{(m-1),\text{ABS+}}(y_{1,o}^n|\tilde{u}_{1,o}^n) \mathbf{W}^{(m-1),\text{ABS+}}(y_{1,e}^n|\tilde{u}_{1,e}^n) \\ &\stackrel{(c)}{=} \max_{\tilde{u}_{2i+1}^n} \mathbf{W}^{(m-1),\text{ABS+}}(y_{1,o}^n|\tilde{u}_{1,o}^n) \mathbf{W}^{(m-1),\text{ABS+}}(y_{1,e}^n|\tilde{u}_{1,e}^n) \\ &= \max_{\tilde{u}_{2i+1}^n, \tilde{u}_{2i+2}^n \in \{0, 1\}} \max_{\tilde{u}_{2i+3}^n} \mathbf{W}^{(m-1),\text{ABS+}}(y_{1,o}^n|\tilde{u}_{1,o}^n) \\ &\quad \cdot \mathbf{W}^{(m-1),\text{ABS+}}(y_{1,e}^n|\tilde{u}_{1,e}^n) \end{aligned}$$

$$\begin{aligned}
&\stackrel{(d)}{=} \max_{\tilde{u}_{2i+1}, \tilde{u}_{2i+2} \in \{0,1\}} \left( \max_{\tilde{u}_{2i+3}^n} \mathbf{W}^{(m-1), \text{ABS+}}(y_{1,o}^n | \tilde{u}_{1,o}^n) \right) \cdot \\
&\quad \cdot \left( \max_{\tilde{u}_{2i+3}^n} \mathbf{W}^{(m-1), \text{ABS+}}(y_{1,e}^n | \tilde{u}_{1,e}^n) \right) \\
&= \max_{\tilde{u}_{2i+1}, \tilde{u}_{2i+2} \in \{0,1\}} \tilde{\mathbf{V}}_i^{(m-1), \text{ABS+}}(y_{1,o}^n, \tilde{u}_{1,o}^{2i-2} | \tilde{u}_{2i-1}, \tilde{u}_{2i+1}) \cdot \\
&\quad \cdot \tilde{\mathbf{V}}_i^{(m-1), \text{ABS+}}(y_{1,e}^n, \tilde{u}_{1,e}^{2i-2} | \tilde{u}_{2i}, \tilde{u}_{2i+2}) \\
&\stackrel{(e)}{=} \max_{u_{2i+1}, u_{2i+2} \in \{0,1\}} \tilde{\mathbf{V}}_i^{(m-1), \text{ABS+}}(y_{1,o}^n, \tilde{u}_{1,o}^{2i-2} | u_{2i-1} + u_{2i}, \\
&\quad u_{2i+1} + u_{2i+2}) \cdot \\
&\quad \cdot \tilde{\mathbf{V}}_i^{(m-1), \text{ABS+}}(y_{1,e}^n, \tilde{u}_{1,e}^{2i-2} | u_{2i}, u_{2i+2}) \\
&= (\tilde{\mathbf{V}}_i^{(m-1), \text{ABS+}})^{\tilde{\diamond}}(y_1^n, \tilde{u}_1^{2i-2} | u_{2i-1}, u_{2i}).
\end{aligned}$$

Here for  $u_1^n \in \{0,1\}^n$  we define  $\tilde{u}_1^n = u_1^n Q_m^{\text{ABS+}}(I_{n/2} \otimes F)$ . In particular, since  $2(i-1) \notin \mathcal{I}_S^{(m)}$ ,  $2i \notin \mathcal{I}^{(m)}$ ,  $2(i+1) \notin \mathcal{I}^{(m)}$ ,

$$\begin{aligned}
\tilde{u}_{2i-1} &= u_{2i-1} + u_{2i}, & \tilde{u}_{2i} &= u_{2i}, \\
\tilde{u}_{2i+1} &= u_{2i+1} + u_{2i+2}, & \tilde{u}_{2i+2} &= u_{2i+2}.
\end{aligned} \tag{29}$$

The equality (a) comes from the fact that  $(Y_{1,o}^n | \tilde{U}_{1,o})$  and  $(Y_{1,e}^n | \tilde{U}_{1,e})$  are independent random variables and (b) is the application of (28). To proof (c), one needs to recall that since  $2i \notin \mathcal{I}_S^{(m)}$  each  $u_{2i+1}^n$  is mapped bijectively to  $\tilde{u}_{2i+1}^n$ , so we can iterate over all possible vectors  $\tilde{u}_{2i+1}^n$ . The equality (d) takes place since the functions  $\tilde{u}_{2i+3}^n \mapsto \mathbf{W}^{(m-1), \text{ABS+}}(y_{1,o}^n | \tilde{u}_{1,o}^n)$  and  $\tilde{u}_{2i+3}^n \mapsto \mathbf{W}^{(m-1), \text{ABS+}}(y_{1,e}^n | \tilde{u}_{1,e}^n)$  (with some fixed  $y_1^n, u_1^{2i}, \tilde{u}_{2i+1}$  and  $\tilde{u}_{2i+2}$ ) use disjoint subvectors of the input vector. The equality (e) is obtained by simple relabeling  $\tilde{u}_{2i+1} \mapsto u_{2i+1} + u_{2i+2}$ ,  $\tilde{u}_{2i+2} \mapsto u_{2i+2}$ . As a final remark, we notice that there is the one-to-one mapping from  $u_1^{2i-2}$  to  $\tilde{u}_1^{2i-2}$  and hence the channels  $\tilde{\mathbf{V}}_{2i-1}^{(m), \text{ABS+}}$  and  $(\tilde{\mathbf{V}}_i^{(m-1), \text{ABS+}})^{\tilde{\diamond}}$  are identical.

Omitting some obvious steps, we show that  $\mathbf{V}_{2i}^{(m), \text{ABS+}} = (\mathbf{V}_i^{(m-1), \text{ABS+}})^{\tilde{\diamond}}$  in the same way using only the fact that  $u_{2i+2}^n$  is bijectively mapped to  $\tilde{u}_{2i+2}^n$ :

$$\begin{aligned}
&\tilde{\mathbf{V}}_{2i}^{(m), \text{ABS+}}(y_1^n, u_1^{2i-1} | u_{2i}, u_{2i+1}) = \\
&= \max_{\tilde{u}_{2i+2}^n} \mathbf{W}^{(m-1), \text{ABS+}}(y_{1,o}^n | \tilde{u}_{1,o}^n) \mathbf{W}^{(m-1), \text{ABS+}}(y_{1,e}^n | \tilde{u}_{1,e}^n) \\
&= \max_{u_{2i+2} \in \{0,1\}} \max_{\tilde{u}_{2i+3}^n} \mathbf{W}^{(m-1), \text{ABS+}}(y_{1,o}^n | \tilde{u}_{1,o}^n) \cdot \\
&\quad \cdot \mathbf{W}^{(m-1), \text{ABS+}}(y_{1,e}^n | \tilde{u}_{1,e}^n) \\
&= \max_{\tilde{u}_{2i+2} \in \{0,1\}} \tilde{\mathbf{V}}_i^{(m-1), \text{ABS+}}(y_{1,o}^n, \tilde{u}_{1,o}^{2i-2} | \tilde{u}_{2i-1}, \tilde{u}_{2i+1}) \cdot \\
&\quad \cdot \tilde{\mathbf{V}}_i^{(m-1), \text{ABS+}}(y_{1,e}^n, \tilde{u}_{1,e}^{2i-2} | \tilde{u}_{2i}, \tilde{u}_{2i+2}) \\
&= \max_{u_{2i+2} \in \{0,1\}} \tilde{\mathbf{V}}_i^{(m-1), \text{ABS+}}(y_{1,o}^n, \tilde{u}_{1,o}^{2i-2} | u_{2i-1} + u_{2i}, \\
&\quad u_{2i+1} + u_{2i+2}) \cdot \\
&\quad \cdot \tilde{\mathbf{V}}_i^{(m-1), \text{ABS+}}(y_{1,e}^n, \tilde{u}_{1,e}^{2i-2} | u_{2i}, u_{2i+2}) \\
&= (\tilde{\mathbf{V}}_i^{(m-1), \text{ABS+}})^{\tilde{\diamond}}(y_1^n, \tilde{u}_1^{2i-1} | u_{2i}, u_{2i+1}).
\end{aligned}$$

To terminate the proof, we show that  $\tilde{\mathbf{V}}_{2i+1}^{(m), \text{ABS+}} = (\tilde{\mathbf{V}}_i^{(m-1), \text{ABS+}})^{\tilde{\Delta}}$  in the way discussed above, taking into

account that since  $2(i+1) \notin \mathcal{I}_S^{(m)}$ , there is the one-to-one mapping from  $u_{2i+3}^n$  to  $\tilde{u}_{2i+3}^n$ :

$$\begin{aligned}
&\tilde{\mathbf{V}}_{2i}^{(m), \text{ABS+}}(y_1^n, u_1^{2i} | u_{2i+1}, u_{2i+2}) = \\
&= \max_{\tilde{u}_{2i+3}^n} \mathbf{W}^{(m-1), \text{ABS+}}(y_{1,o}^n | \tilde{u}_{1,o}^n) \mathbf{W}^{(m-1), \text{ABS+}}(y_{1,e}^n | \tilde{u}_{1,e}^n) \\
&= \tilde{\mathbf{V}}_i^{(m-1), \text{ABS+}}(y_{1,o}^n, \tilde{u}_{1,o}^{2i-2} | \tilde{u}_{2i-1}, \tilde{u}_{2i+1}) \cdot \\
&\quad \cdot \tilde{\mathbf{V}}_i^{(m-1), \text{ABS+}}(y_{1,e}^n, \tilde{u}_{1,e}^{2i-2} | \tilde{u}_{2i}, \tilde{u}_{2i+2}) \\
&= \tilde{\mathbf{V}}_i^{(m-1), \text{ABS+}}(y_{1,o}^n, \tilde{u}_{1,o}^{2i-2} | u_{2i-1} + u_{2i}, u_{2i+1} + u_{2i+2}) \cdot \\
&\quad \cdot \tilde{\mathbf{V}}_i^{(m-1), \text{ABS+}}(y_{1,e}^n, \tilde{u}_{1,e}^{2i-2} | u_{2i}, u_{2i+2}) \\
&= (\tilde{\mathbf{V}}_i^{(m-1), \text{ABS+}})^{\tilde{\Delta}}(y_1^n, \tilde{u}_1^{2i} | u_{2i+1}, u_{2i+2}).
\end{aligned}$$

Finally, we are to discuss the remaining cases of the lemma. The cases (i)-(ii) can be proven in the same way up to replacing (29) with a corresponding relation between  $u_{2i-1}^{2i+2}$  and  $\tilde{u}_{2i-1}^{2i+2}$ . Meanwhile, the cases (iii)-(v) have already been proven. Indeed, while proving  $\tilde{\mathbf{V}}_{2i-1}^{(m), \text{ABS+}} = (\tilde{\mathbf{V}}_i^{(m-1), \text{ABS+}})^{\tilde{\nabla}}$  we did not use  $2(i+1) \notin \mathcal{I}^{(m)}$  (we did not use even  $\tilde{u}_{2i+1} = u_{2i+1} + u_{2i+2}$ ,  $\tilde{u}_{2i+2} = u_{2i+2}$  from (29): instead, we did a bijective substitution for the "free" variables  $\tilde{u}_{2i+1}$  and  $\tilde{u}_{2i+2}$ ); while proving  $\tilde{\mathbf{V}}_{2i+1}^{(m), \text{ABS+}} = (\tilde{\mathbf{V}}_i^{(m-1), \text{ABS+}})^{\tilde{\Delta}}$  we did not use  $2(i-1) \notin \mathcal{I}_S^{(m)}$  and while proving  $\tilde{\mathbf{V}}_{2i}^{(m), \text{ABS+}} = (\tilde{\mathbf{V}}_i^{(m-1), \text{ABS+}})^{\tilde{\diamond}}$  we did not use neither of those statements.

## REFERENCES

- [1] E. Arikan, "Channel polarization: A method for constructing capacity-achieving codes for symmetric binary-input memoryless channels," *IEEE Transactions on Information Theory*, vol. 55, no. 7, pp. 3051–3073, 2009.
- [2] I. Tal and A. Vardy, "List decoding of polar codes," *IEEE Transactions on Information Theory*, vol. 61, no. 5, pp. 2213–2226, 5 2015.
- [3] C. Y. Xia, J. Chen, Y. Z. Fan, C. ying Tsui, J. Jin, H. Shen, and B. Li, "A high-throughput architecture of list successive cancellation polar codes decoder with large list size," *IEEE Transactions on Signal Processing*, vol. 66, no. 4, 7 2018.
- [4] M. Mondelli, S. H. Hassani, and R. Urbanke, "Scaling exponent of list decoders with applications to polar codes," *IEEE Transactions On Information Theory*, vol. 61, no. 9, 9 2015.
- [5] V. Miloslavskaya and P. Trifonov, "Sequential decoding of polar codes," *IEEE Communications Letters*, vol. 18, no. 7, pp. 1127–1130, 2014.
- [6] C. Pillet, I. Sagitov, D. Deslandes, and P. Giard, "Successive-cancellation flip and perturbation decoder of polar codes," in *Proceedings of IEEE Wireless Communications and Networking Conference (WCNC)*, 2025, pp. 1–6.
- [7] S. A. Hashemi, C. Condo, and W. J. Gross, "List sphere decoding of polar codes," in *2015 49th Asilomar Conference on Signals, Systems and Computers*, 2015, pp. 1346–1350.
- [8] E. Arikan, "Polar codes: A pipelined implementation," in *Proceedings of the 4th International Symposium on Broadband Communnication*, 2010, pp. 11–14.
- [9] M. Kamenev, Y. Kameneva, O. Kurmaev, and A. Maevskiy, "Permutation decoding of polar codes," in *Proceedings of XVI International Symposium*, 2019.
- [10] P. Trifonov, "Design and decoding of polar codes with large kernels: a survey," *Problems of Information Transmission*, vol. 59, no. 1, pp. 22–40, 2023.
- [11] S. B. Korada, E. Sasoglu, and R. Urbanke, "Polar codes: Characterization of exponent, bounds, and constructions," *IEEE Transactions on Information Theory*, vol. 56, no. 12, pp. 6253–6264, 12 2010.
- [12] G. Trofimuk and P. Trifonov, "Construction of binary polarization kernels for low complexity window processing," in *Proceedings of IEEE Information Theory Workshop*, 2019.
- [13] G. Trofimuk and P. Trifonov, "Window processing of binary polarization kernels," *IEEE Transactions on Communications*, vol. 69, no. 7, pp. 4294–4305, July 2021.
- [14] G. Li, M. Ye, and S. Hu, "Adjacent-bits-swapped polar codes: A new code construction to speed up polarization," *IEEE Transactions on Information Theory*, vol. 69, no. 4, pp. 2269–2299, Apr. 2023.
- [15] ———, "Abs+ polar codes: Exploiting more linear transforms on adjacent bits," *IEEE Transactions on Information Theory*, vol. 70, no. 2, pp. 1067–1086, 2024.
- [16] A. Balatsoukas-Stimming, M. B. Parizi, and A. Burg, "LLR-based successive cancellation list decoding of polar codes," *IEEE Transactions On Signal Processing*, vol. 63, no. 19, pp. 5165–5179, 10 2015.
- [17] S. A. Hashemi, C. Condo, and W. Gross, "Fast and flexible successive-cancellation list decoders for polar codes," *IEEE Transactions on Signal Processing*, vol. 65, no. 1, 2017.
- [18] C. Leroux, I. Tal, A. Vardy, and W. Gross, "Hardware architectures for successive cancellation decoding of polar codes," in *Proceedings of IEEE International Conference on Acoustics, Speech and Signal Processing*, 5 2011, pp. 1665–1668.
- [19] A. Alamdar-Yazdi and F. Kschischang, "A simplified successive-cancellation decoder for polar codes," *IEEE Communications Letters*, vol. 15, no. 12, 12 2011.